



OPEN ACCESS

EDITED BY
Shihui Yang,
Hubei University, China

REVIEWED BY
Binan Geng,
Hubei University, China
Marina Sheremetieva,
National Research Center Kurchatov
Institute, Russia

*CORRESPONDENCE
Nadja A. Henke,
✉ nadja.henke@kit.edu

RECEIVED 10 March 2026
REVISED 14 April 2026
ACCEPTED 23 April 2026
PUBLISHED 26 May 2026

CITATION

Will PM, Göttl VL, Seeger J, Wendisch VF and Henke NA (2026) Design and validation of an inducible and curable EvolvR system for directed evolution in *Corynebacterium glutamicum*. *Front. Bioeng. Biotechnol.* 14:1827071. doi: 10.3389/fbioe.2026.1827071

COPYRIGHT

© 2026 Will, Göttl, Seeger, Wendisch and Henke. This is an open-access article distributed under the terms of the [Creative Commons Attribution License \(CC BY\)](https://creativecommons.org/licenses/by/4.0/). The use, distribution or reproduction in other forums is permitted, provided the original author(s) and the copyright owner(s) are credited and that the original publication in this journal is cited, in accordance with accepted academic practice. No use, distribution or reproduction is permitted which does not comply with these terms.

Design and validation of an inducible and curable EvolvR system for directed evolution in *Corynebacterium glutamicum*

Paul M. Will¹, Vanessa L. Göttl¹, Jan Seeger¹, Volker F. Wendisch¹ and Nadja A. Henke^{2*}

¹Genetics of Prokaryotes, CeBiTec and Faculty of Biology, Bielefeld University, Bielefeld, Germany,

²Institute of Process Engineering in Life Sciences, Department of Chemical and Process Engineering, Karlsruhe Institute of Technology, Karlsruhe, Germany

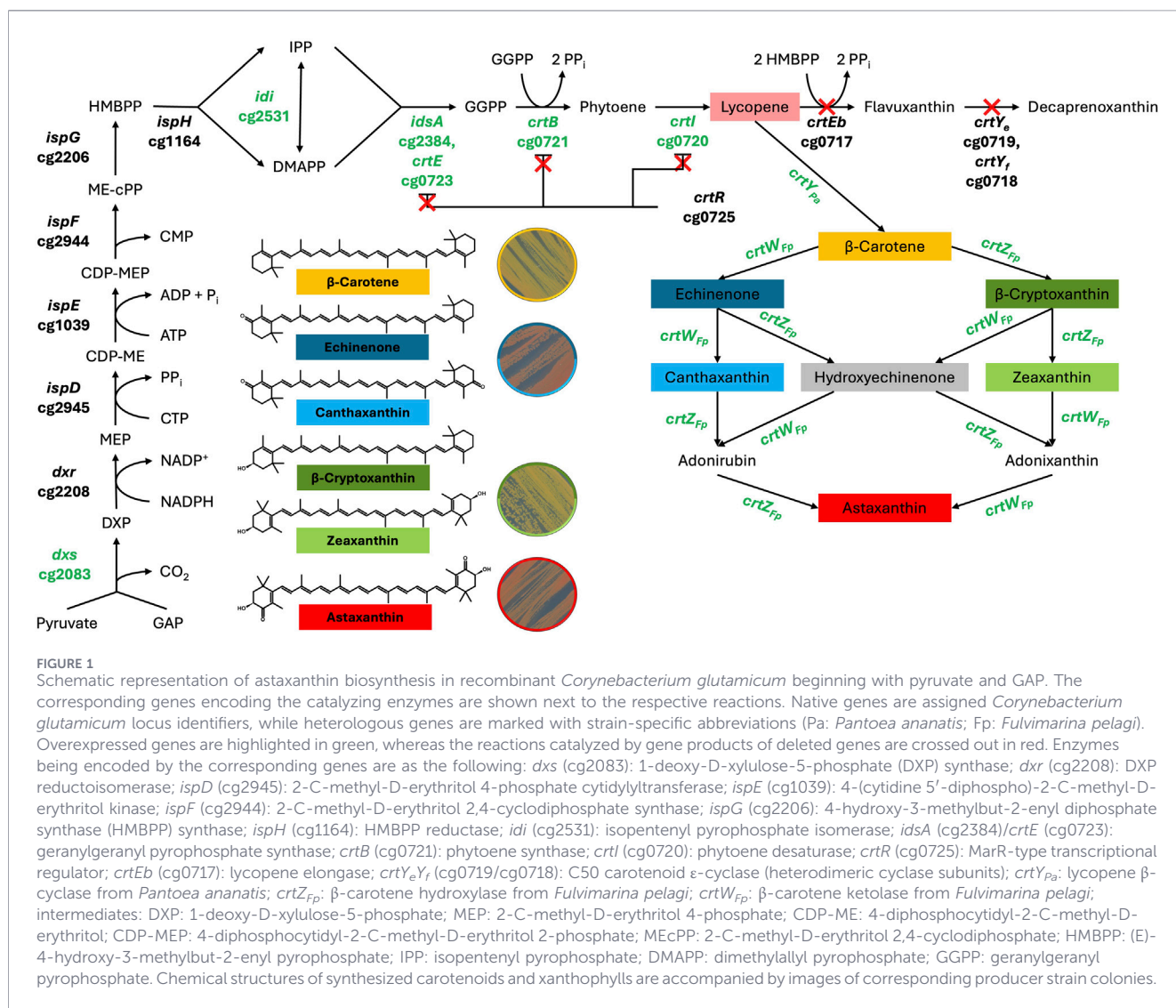
The EvolvR system was developed as a tool for the continuous diversification of user-defined genomic loci in *Escherichia coli*. To make EvolvR accessible for enzyme engineering in *Corynebacterium glutamicum*, this work focused on the design and construction of gpEvolvR — a modified plasmid active in both *Escherichia coli* and *Corynebacterium glutamicum* with additional recombinant features enabling its complete curing after mutagenesis. First, the pSC101 origin of replication of gpEvolvR itself served as the proof-of-principle mutagenesis target. Two examined *E. coli* mutants exhibited substantial increases in kanamycin minimal inhibitory concentrations of +44% and +96% and thus confirmed the functionality of the new gpEvolvR plasmid system. Secondly, the EvolvR-based directed evolution of a genomically located gene was shown in *C. glutamicum*. Given that the β -carotene ketolase (CrtW) has been identified as a key optimization target in previous metabolic engineering studies of *C. glutamicum*, EvolvR was successfully applied to generate mutants with varying activities, which were identified through plate-based screening. Although none of the examined *crtW* mutants outperformed the reference sequence in production experiments, this study introduced the newly constructed and curable EvolvR system as a tool for targeted hypermutation in *C. glutamicum*.

KEYWORDS

carotenoids, *Corynebacterium glutamicum*, directed evolution, EvolvR, plasmid design

1 Introduction

Industrial biotechnology has become a key pillar of modern production of bulk chemicals and other value-added compounds. *Corynebacterium glutamicum* is a well-established cell factory in white biotechnology, famous for its large-scale production of the amino acids L-glutamate and L-lysine (Wendisch, 2020). Moreover *C. glutamicum* is a natural producer of the carotenoid decaprenoxanthin, giving it its yellow pigmentation (Hayashi et al., 2018; Heider et al., 2012; Henke et al., 2017; Sandmann, 1994; Stegelmann et al., 2026). In response to the rising demand for carotenoids and xanthophylls within the industry (Berman et al., 2015), the natural pathway was modified to access the high-value product astaxanthin with this organism (Figure 1) (Henke et al., 2016). Platform strain engineering was conducted applying different metabolic engineering strategies in order to transform *C. glutamicum* into a producer of the central carotenoid lycopene (Heider et al., 2014; Heider et al., 2012). To expand the production portfolio towards astaxanthin, the



expression of three heterologous genes was required. Branching off from lycopene, its cyclization into the orange carotenoid β-carotene was enabled by the expression of a lycopene cyclase (*CrtY_{pa}*) encoded by the *crtY_{pa}* gene from *Pantoea ananatis* (Heider et al., 2014). Finally, astaxanthin production was established by additional expression of a β-carotene ketolase (*CrtW*) and a β-carotene hydroxylase (*CrtZ*) encoded by the respective genes *crtW_{Fp}* and *crtZ_{Fp}* from *Fulvimarina pelagi* (Henke et al., 2016). The fusion of *CrtZ_{Fp}* and *CrtW_{Fp}* (*CrtZ_{Fp}* ~ *CrtW_{Fp}*) via a flexible linker (Henke and Wendisch, 2019) balanced astaxanthin production in *C. glutamicum* (Göttl et al., 2024). However, complete β-carotene conversion could not be achieved, suggesting bottlenecks in the reactions catalyzed by β-carotene ketolase (*CrtW_{Fp}*) and β-carotene hydroxylase (*CrtZ_{Fp}*) as similar reported for astaxanthin biosynthesis in other microbial hosts (Lu et al., 2017; Zhang et al., 2022).

Metabolic engineering and enzyme optimization are central strategies to improve product titers and expand the product portfolio of microorganisms for useful purposes. Classical enzyme

engineering strategies such as random mutagenesis do not rely on sequence-structure-function understanding. However, such approaches are limited in terms of library size, specificity and labor intensities (Bornscheuer et al., 2012; Packer and Liu, 2015). Especially the last aspect can be addressed with *in vivo* approaches, that require only initial setup for autonomous operation. Besides more traditional *in vivo* mutagenesis protocols that induce DNA damage using chemical mutagens or physical irradiation, mutator strains with defective DNA repair systems served as safer alternatives for genome-wide mutagenesis. As sequencing became broadly affordable (Shendure and Aiden, 2012), many databases and tools have contributed to a much better understanding of the sequence-structure-function relationship of encoded proteins (Kewalramani et al., 2023; Kroll et al., 2023; Pereira and Alva, 2021). Today, prediction of the impact of mutations is accelerated by artificial intelligence and combined with omics technologies, which allows for precise interventions into cellular metabolism (Fletcher et al., 2022). Over the past years the repertoire of available *in vivo* genetic engineering techniques for the precise alteration of DNA sequences has

expanded significantly. Zinc Finger Nucleases (ZFN) (Kim et al., 1996) and Transcription Activator-Like Effector Nucleases (TALENs) (Boch et al., 2009) were recently surpassed by editing via clustered regularly interspaced short palindromic repeats (CRISPR). Modern CRISPR gene editing only requires cloning of a suitable protospacer upstream of a crRNA-tracrRNA fusion transcript to create an expressible sgRNA, which serves as a targeting handle for the CRISPR-associated (Cas) nuclease (Jinek et al., 2012; Mali et al., 2013). This sgRNA-nuclease complex specifically targets and cleaves double-stranded DNA at nuclease-specific protospacer adjacent motifs (PAM) (Mojica et al., 2009). Beyond double-strand nucleases for insertions and deletions, nicking nucleases (nCas) that create single-strand breaks (Cong et al., 2013) and catalytically dead versions (dCas) that retain targeting ability without cleavage (Qi et al., 2013) are established. These variants exploit the precise targeting capabilities of Cas proteins for diverse applications, including repression of gene expression (Göttl et al., 2021; Schultenkämper et al., 2019).

The EvolvR system is known as a technique combining aspects of random mutagenesis and rational design for the evolution of enzymes through diversification of user-defined loci in *E. coli* (Halperin et al., 2018). By fusing an enhanced Cas9 nickase (enCas9) (Slaymaker et al., 2016) to the N-terminus of a DNA polymerase I in which several introduced mutations led to a low-fidelity phenotype (Poll5M) (Camps et al., 2003; Loh et al., 2010), a CRISPR-guided error-prone DNA polymerase was generated for the mutagenesis of targeted regions. Thus, EvolvR can be understood as a hybrid approach combining elements of randomized mutagenesis and rational design. The concept of the EvolvR system (Halperin et al., 2018) operates as the following: (i) the DNA strand complementary to the co-expressed sgRNA (complementary strand) is nicked three base pairs upstream of the PAM, mediated by the Cas9 nuclease variant with a D10A mutation in the RuvC-like domain (enCas9) (Jinek et al., 2012), (ii) dissociation of the nickase (enCas9) from the DNA, (iii) the fused error-prone DNA polymerase (Poll5M) binds to the nick and performs mutagenic strand-displacement DNA synthesis, (iv) the displaced strand is then cleaved and degraded by the intrinsic flap endonuclease activity of the DNA polymerase, (v) the remaining nick is ligated by the endogenous DNA repair system.

Adaptive laboratory evolution (ALE) arose as a technique to mimic natural evolution in a laboratory setting by applying strong to lethal selective pressure (Elena and Lenski, 2003), e.g., forcing *C. glutamicum* cells to adapt to certain conditions such as the utilization of novel carbon sources (Werner et al., 2023) or the increasing tolerance towards toxic compounds and inhibitors (Leßmeier and Wendisch, 2015; Wang X. et al., 2018). Although EvolvR poses a powerful tool to enhance ALE processes in a continuous directed evolution (CDE) format by introducing additional variance into targeted relevant regions, it can also be applied without additional selective pressure. Together with a suitable screening method substituting for natural selection, this can allow for the directed evolution of enzymes whose products (e.g., carotenoids) could not be subjected to conventional ALE before.

However, this would require the possibility to halt the mutagenic process of EvolvR to ensure a stable relationship between genotype and phenotype for a subsequent mutant characterization via screening and gene sequencing. Although the expression of the EvolvR fusion protein from the pEvolvR-*enCas9-poll5M* plasmid

can be induced by anhydrotetracycline (aTc), it cannot be stopped. Therefore, a proper curing process needs to be established to allow the use of the EvolvR system in such a directed evolution scenario. Furthermore, EvolvR was developed for *E. coli* and has already been adapted to yeast (Tou et al., 2020) and mammalian cells (Hurtado et al., 2025), but has not yet been transferred to the industrial workhorse *C. glutamicum*.

The aim of this study was to construct a dual-inducible and curable EvolvR-based plasmid-borne system that allows for the targeted mutagenesis in the industrial workhorses *C. glutamicum* and *E. coli*. The core value of the established system allows the rapid generation of mutant libraries in *C. glutamicum* without extensive *in vitro* cloning effort. Moreover, when combined with ALE and suitable screening assays, it can accelerate the design of enzyme properties in academic and applied research.

2 Materials and methods

2.1 General cultivation conditions of *E. coli* and *C. glutamicum*

E. coli and *C. glutamicum* cultures (Table 1) were cultivated in volumes of 10 mL or 50 mL in 100 mL or 500 mL baffled flasks, respectively. *E. coli* was incubated in an Ecotron shaker (Infors HT, Bottmingen, Switzerland) at 180 rpm and 37 °C. *C. glutamicum* cultures were incubated in a climate chamber at 120 rpm (corresponding to 0.402 × g) and 30 °C. Where applicable, cultures containing plasmids were supplemented with vector-specific antibiotics tetracycline (5 µg mL⁻¹), kanamycin (25 µg mL⁻¹), chloramphenicol (7.5 µg mL⁻¹) (VWR International GmbH, Darmstadt, Germany) to maintain selective pressure.

2.2 General cloning strategy

Molecular cloning was performed via Gibson assembly (Gibson et al., 2009). In brief, target DNA fragments were amplified with a High-Fidelity DNA Polymerase (Allin™, highQu GmbH, Kraichtal, Germany). To enhance amplification efficiency dimethyl sulfoxide (DMSO) and betaine were added to the reaction mix. Plasmids were isolated from *E. coli* DH5α 10 mL or 50 mL overnight LB cultures (plus appropriate antibiotics) using the QIAwave Plasmid Miniprep Kit (QIAGEN GmbH, Hilden, Germany) according to the manufacturer's protocol. Plasmids were linearized with the respective restriction enzyme (Thermo Fisher Scientific Baltics UAB, Vilnius, Lithuania) and subsequently dephosphorylated with Antarctic Phosphatase (New England Biolabs GmbH, Frankfurt, Germany). PCR products and restricted plasmids were purified either from suspension or agarose-gels by using the NucleoSpin™ Gel and PCR Clean-Up Kit (Macherey-Nagel GmbH & Co. KG, Düren, Germany). Linearized plasmids and insert DNA were used for the Gibson assembly (Gibson et al., 2009). Chemically competent *E. coli* DH5α cells were used for subcloning of all new plasmid constructs (Table 2), that were subsequently tested by colony PCR (cPCR). Sequencing of DNA was either performed as Sanger sequencing at the Sequencing Core Facility in the Center for Biotechnology at Bielefeld University

TABLE 1 Plasmids used in this study.

Plasmid	Features	References
pECXT-P _{Syn} - <i>crtW</i> _{FP}	Tet ^R , pEC-XT99A-P _{Syn} derivative for constitutive expression of <i>crtW</i> from <i>F. pelagi</i> under the control of the synthetic P _{Syn} promoter (Rytter et al., 2014)	Göttl et al. (2024)
pECXT-P _{tuf} - <i>crtW</i> _{FP}	Tet ^R , pEC-XT99A-P _{tuf} derivative for constitutive expression of <i>crtW</i> from <i>F. pelagi</i> under the control of the P _{tuf} promoter from <i>C. glutamicum</i>	This work
pK19 <i>mobsacB</i>	pK18 (oriV _{Ec} , <i>sacB</i> , <i>lacZ_α</i>) Km ^R , <i>C. glutamicum</i> / <i>E. coli</i> expression shuttle vector for construction of genomic insertion and deletion mutants of <i>C. glutamicum</i>	Schäfer et al. (1994)
pK19 <i>mobsacB</i> Δ <i>actA</i> ::P _{H36} - <i>crtW</i> _{FP}	Km ^R , pK19 <i>mobsacB</i> derivative for the deletion of the <i>actA</i> locus and integration of the <i>crtW</i> gene from <i>F. pelagi</i> under the control of the P _{H36} promoter (Yim et al., 2013)	This work
pK19 <i>mobsacB</i> Δ <i>actA</i> ::P _{tuf} - <i>crtW</i> _{FP}	Km ^R , pK19 <i>mobsacB</i> derivative for the deletion of the <i>actA</i> locus and integration of the <i>crtW</i> gene from <i>F. pelagi</i> under the control of the P _{tuf} promoter from <i>C. glutamicum</i>	This work
pK19 <i>mobsacB</i> Δ <i>actA</i> ::P _{Syn} - <i>crtW</i> _{FP}	Km ^R , pK19 <i>mobsacB</i> derivative for the deletion of the <i>actA</i> locus and integration of the <i>crtW</i> gene from <i>F. pelagi</i> under the control of the P _{Syn} promoter	This work
pEvolvR- <i>enCas9-poli5M</i>	Km ^R , oriV _{Ec} , contains translational fused enCas9 nickase and PolI5M (<i>E. coli</i> DNA polymerase I harboring D424A, I709N, A759R, F742Y and P796H mutations) followed by the synthetic L3S2P55 terminator, sgRNA expression cassette	Halperin et al. (2018), Addgene Plasmid #113078
pSH1	Km ^R , P _{tuf} , pHM519 oriV _{Cg} , <i>C. glutamicum</i> / <i>E. coli</i> expression shuttle vector	Henke et al. (2016)
pSH1-EvolvR	Km ^R , pSH1 derivative containing <i>Sall</i> and <i>PstI</i> cured <i>enCas9-poli5M</i> sequence	This work
pJYS3_easy cloning	Km ^R , pJYS3_Δ <i>crtY_{ef}</i> (Jiang et al., 2017) derivative; Km ^R , repA101, pSC101 ori <i>E. coli</i> replicon, pBL1 _{ts} temperature sensitive <i>C. glutamicum</i> replicon, <i>cpfI</i> nuclease from <i>Francisella novicida</i> under the control of the constitutive P _{lacM} promoter, rrmB T ₂ Terminator	This work
pS_dCas9	Cm ^R , pRG_dCas9 (Gauttam et al., 2019) derivative carrying the Cas9 handle followed by the terminator from <i>Streptococcus pyogenes</i> amplified from the piCas plasmid (Schultenkämper et al., 2019)	Göttl et al. (2021)
gpEvolvR	Km ^R , repA101, pSC101 ori <i>E. coli</i> replicon, pBL1 _{ts} temperature sensitive <i>C. glutamicum</i> replicon, <i>tetO/tetR</i> regulated expression of <i>Sall</i> and <i>PstI</i> cured <i>enCas9-poli5M</i> sequence, <i>lacI^f</i> inducible sgRNA scaffold	This work
gpEvolvR -HIS ₁	Km ^R , gpEvolvR derivative containing a 20bp protospacer targeting the area upstream of the first conserved histidine rich region within the <i>crtW</i> gene from <i>F. pelagi</i>	This work
gpEvolvR -HIS _{1,2}	Km ^R , gpEvolvR derivative containing a 20bp protospacer targeting the area upstream between the first and second conserved histidine rich region within the <i>crtW</i> gene from <i>F. pelagi</i>	This work

(Continued)

TABLE 1 Continued

Plasmid	Features	References
gpEvolvR -HIS ₃	Km ^R , gpEvolvR derivative containing a 20bp protospacer targeting the area upstream of the third conserved histidine rich region within the <i>crtW</i> gene from <i>F. pelagi</i>	This work
pSH1- <i>crtW</i> _{FP} +MX	Km ^R , pSH1 derivative containing a <i>crtW</i> _{FP} variant	This work
gpEvolvR-ORI ₂	Km ^R , gpEvolvR derivative containing a 20bp protospacer targeting the pSC101 ori within gpEvolvR	This work
gpEvolvR-ORI ₂ ^{X1}	Km ^R , gpEvolvR derivative containing a 20bp protospacer targeting the pSC101 ori within gpEvolvR harboring a T318A SNP in the pSC101 ori	This work
gpEvolvR-ORI ₂ ^{X9}	Km ^R , gpEvolvR derivative containing a 20bp protospacer targeting the pSC101 ori within gpEvolvR harboring a T395C SNP in the pSC101 ori	This work

(Bielefeld, Germany) or as Oxford Nanopore Technologies (ONT) sequencing externally at Microsynth SeqLab GmbH (Göttingen, Germany).

2.3 Construction of the gpEvolvR plasmid

As protospacer integration was aimed for at *PstI* or *SalI* sites in the new construct, undesired restriction motifs had to be removed from affected sequences. For this purpose, a 7,754 bp fragment of the plasmid pEvolvR-*enCas9-pollI5M* (Halperin et al., 2018) (Addgene Plasmid #113078), comprising *tetR*, *enCas9-pollI5M*, and other regulatory elements, was divided into three fragments. The first fragment, containing *tetR* and part of the *enCas9* sequence, was synthesized as a 1156 bp gene fragment (Twist Bioscience, San Francisco, United States) with both internal *SalI* sites removed. The synthesized fragment was then flanked with matching overhangs by high-fidelity PCR using primers 037P and 038P. The second (5507 bp) and third (1091 bp) fragment were amplified via high-fidelity PCR using primers 039P/040P and 041P/042P, respectively, with primers 040P and 041P introducing the necessary mismatches for the removal of an internal *PstI* site by single nucleotide substitution. All three fragments were stored by assembly into the pSH1 backbone yielding the construct pSH1-EvolvR. For construction of gpEvolvR, the insert of pSH1-EvolvR (043P/044P) as well as the *lacI*^P regulated sgRNA scaffold from pS_dCas9 (045P/046P) and *kanR*, pBL1_{ts}, pSC101 ori and *repA101* from pJYS3_{easy} cloning (047P/048P) were amplified and assembled.

2.4 Protospacer integration into the gpEvolvR system

Suitable protospacers were identified employing *CRISPy-web* (crispy.secondarymetabolites.org) (Blin et al., 2016) with the corresponding host genome as reference to minimize potential off-target effects. Protospacer inserts were generated by the annealing of two complementary oligonucleotides (Sigma-Aldrich Chemie GmbH, Taufkirchen, Deutschland) (ORI₂: 068P/069P;

HIS₁: 083P/084P; HIS₁₋₂: 085P/086P; HIS₃: 089P/090P). 5 μL of each equimolar oligonucleotide solution (100 μM) was added to 990 μL of annealing buffer. The resulting mixture was heated to 95 °C for 5 min and then gradually cooled to room temperature. Subsequently annealed oligonucleotides were assembled into the *PstI*-restricted and dephosphorylated gpEvolvR backbone via Gibson assembly (Gibson et al., 2009). Successful protospacer integration was verified via cPCR and confirmed by Sanger sequencing using the primers *vgai/076P*.

2.5 *In vivo* mutagenesis of the pSC101 ori by gpEvolvR in *E. coli*

A 10 mL LB_{Km25} overnight culture of *E. coli* DH5α (gpEvolvR-ORI₂), inoculated from a glycerol stock, was diluted to an OD_{600nm} of 0.02 using sterile LB medium. Subsequently, 100 μL of the diluted cell suspension were plated onto LB agar plates containing 500 μg mL⁻¹ kanamycin, 0.25 μg mL⁻¹ anhydrotetracycline (aTc), and 1 mM isopropyl-β-D-thiogalactopyranoside (IPTG). Plates were incubated at 37 °C for approximately 24 h. After incubation, individual colonies were transferred to LB_{Km1000} agar plates to isolate clones, apply higher selective pressure, and remove the inducers to stop the mutagenic process.

The targeted pSC101 ori (029P/097P) and the kanamycin resistance cassette (*kanR*) including 250 bp upstream regulatory elements (035P/091P) were amplified via cPCR. Amplicons were treated with ExoSAP-IT™ (Applied Biosystems™, Thermo Fisher Scientific, Waltham, USA) and subjected to Sanger sequencing using primers 029P and 097P for the pSC101 ori, and 035P, 036P, 091P, and 100P for *kanR*. Clones containing unique *de novo* mutations in the pSC101 ori but no mutations within the amplified *kanR* region were selected and preserved as glycerol stocks for further experiments.

Overnight precultures of *E. coli* strains were harvested by centrifugation at 4,000 × g for 7 min and washed twice with TN buffer. The cell pellet was resuspended in 1 mL LB medium to an OD_{600nm} of 1.0 using a V-1200 spectrophotometer (VWR International bvba, Leuven, Belgium). For each well of a

TABLE 2 Strains used in this study.

Strain	Features	References
<i>E. coli</i> strains		
<i>E. coli</i> DH5α	F ⁻ endA1 hsdR17 (r _k ,m ⁺ k) supE44 thi-1 λ ⁻ recA1 gyrA96 relA1 deoR Δ(lacZYA-argF)-U169φ 80dlacZΔM15	Hanahan (1983)
<i>E. coli</i> DH5α (gpEvolvR-ORI ₂)	<i>E. coli</i> DH5α derivative containing the gpEvolvR-ORI ₂ plasmid	This work
<i>E. coli</i> DH5α (gpEvolvR-ORI ₂ ^{X1})	<i>E. coli</i> DH5α derivative containing the gpEvolvR-ORI ₂ ^{X1} plasmid	This work
<i>E. coli</i> DH5α (gpEvolvR-ORI ₂ ^{X9})	<i>E. coli</i> DH5α derivative containing the gpEvolvR-ORI ₂ ^{X9} plasmid	This work
<i>E. coli</i> DH5α (pVWEx1)	<i>E. coli</i> DH5α derivative containing the pVWEx1 plasmid	Peters-Wendisch et al. (2001)
<i>C. glutamicum</i> strains		
<i>C. glutamicum</i> BETA4	<i>C. glutamicum</i> MB001 derivative producing β-carotene	Henke et al. (2016)
<i>C. glutamicum</i> BETA4 (pSH1- <i>crtW</i> _{P_{in}})	<i>C. glutamicum</i> BETA4 derivative containing the pSH1- <i>crtW</i> _{P_{in}} plasmid for constitutive expression of codon optimized <i>crtW</i> encoding for CrtW from <i>Paracoccus</i> N81106 with M99I/L175M mutations	This work
<i>C. glutamicum</i> BETA4 (pSH1- <i>crtW</i> _{S_d})	<i>C. glutamicum</i> BETA4 derivative containing the pSH1- <i>crtW</i> _{P_{in}} plasmid for constitutive expression of codon optimized <i>crtW</i> encoding for CrtW from <i>Sphingomonas</i> DC18 with R203W/F213L mutations	This work
<i>C. glutamicum</i> BETA4 (pSH1- <i>crtW</i> _{F_p})	<i>C. glutamicum</i> BETA4 derivative containing the pSH1- <i>crtW</i> _{F_p} plasmid for constitutive expression of <i>crtW</i> from <i>Fulvimarina pelagi</i>	Henke et al. (2016)
<i>C. glutamicum</i> BETA4 Δ <i>actA</i> ::P _{H36} - <i>crtW</i> _{F_p}	<i>C. glutamicum</i> BETA4 derivative with integration of the <i>crtW</i> _{F_p} into the <i>actA</i> (cg2840) locus of the <i>C. glutamicum</i> genome for constitutive expression under control of the P _{H36} promoter	This work
<i>C. glutamicum</i> BETA4 Δ <i>actA</i> ::P _{tuf} - <i>crtW</i> _{F_p}	<i>C. glutamicum</i> BETA4 derivative with integration of the <i>crtW</i> _{F_p} into the <i>actA</i> (cg2840) locus of the <i>C. glutamicum</i> genome for constitutive expression under control of the P _{tuf} promoter	This work
<i>C. glutamicum</i> BETA4 Δ <i>actA</i> ::P _{Syn} - <i>crtW</i> _{F_p}	<i>C. glutamicum</i> BETA4 derivative with integration of the <i>crtW</i> _{F_p} into the <i>actA</i> (cg2840) locus of the <i>C. glutamicum</i> genome for constitutive expression under control of the P _{Syn} promoter	This work
<i>C. glutamicum</i> BETA4 Δ <i>actA</i> ::P _{Syn} - <i>crtW</i> _{F_p} (gpEvolvR-HIS ₁)	<i>C. glutamicum</i> BETA4 derivative with P _{Syn} - <i>crtW</i> _{F_p} integrated into the <i>actA</i> (cg2840) locus of the <i>C. glutamicum</i> genome harboring the gpEvolvR-HIS ₁ plasmid for mutagenesis of <i>crtW</i> _{F_p}	This work
<i>C. glutamicum</i> BETA4 Δ <i>actA</i> ::P _{Syn} - <i>crtW</i> _{F_p} (gpEvolvR-HIS ₁₋₂)	<i>C. glutamicum</i> BETA4 derivative with P _{Syn} - <i>crtW</i> _{F_p} integrated into the <i>actA</i> (cg2840) locus of the <i>C. glutamicum</i> genome harboring the gpEvolvR-HIS ₁₋₂ plasmid for mutagenesis of <i>crtW</i> _{F_p}	This work
<i>C. glutamicum</i> BETA4 Δ <i>actA</i> ::P _{Syn} - <i>crtW</i> _{F_p} (gpEvolvR-HIS ₃)	<i>C. glutamicum</i> BETA4 derivative with P _{Syn} - <i>crtW</i> _{F_p} integrated into the <i>actA</i> (cg2840) locus of the <i>C. glutamicum</i> genome harboring the gpEvolvR-HIS ₃ plasmid for mutagenesis of <i>crtW</i> _{F_p}	This work
<i>C. glutamicum</i> BETA4 (pSH1- <i>crtW</i> _{F_p} *MX)	<i>C. glutamicum</i> BETA4 derivative containing a pSH1- <i>crtW</i> _{F_p} *MX plasmid	This work
<i>C. glutamicum</i> BETA4 (pECXT-P _{Syn} - <i>crtZ</i> _{F_p})	<i>C. glutamicum</i> BETA4 derivative containing a pECXT-P _{Syn} - <i>crtZ</i> _{F_p} plasmid for constitutive expression of the <i>crtZ</i> gene from <i>F. pelagi</i>	Meyer et al. (2025)
<i>C. glutamicum</i> BETA4 (pECXT-P _{Syn} - <i>crtZ</i> _{F_p}) (pSH1- <i>crtW</i> _{F_p})	<i>C. glutamicum</i> BETA4 derivative containing both plasmids pECXT-P _{Syn} - <i>crtZ</i> _{F_p} and pSH1- <i>crtW</i> _{F_p} for constitutive expression of both genes <i>crtZ</i> and <i>crtW</i> from <i>F. pelagi</i>	This work
<i>C. glutamicum</i> BETA4 (pSH1- <i>crtW</i> _{F_p} *MX) (pECXT-P _{Syn} - <i>crtZ</i> _{F_p})	<i>C. glutamicum</i> BETA4 derivative containing both plasmids pSH1- <i>crtW</i> _{F_p} *MX and pECXT-P _{Syn} - <i>crtZ</i> _{F_p}	This work

flat-bottom 24-well microtiter plate equipped with a CR1224b sandwich cover (System Duetz, EnzyScreen BV, Heemstede, Netherlands), 990 μL of LB medium containing the appropriate antibiotics were mixed with 110 μL of the prepared cell suspension. To determine the initial cell density (t_0), 100 μL of culture were withdrawn from each well for $\text{OD}_{600\text{nm}}$ measurement, leaving 1 mL in each well. Cultivation was carried out in an Ecotron shaker (Infors HT, Bottmingen, Switzerland) at 180 rpm and 37 °C for 24 h.

2.6 *In vivo* mutagenesis of *crtW_{Fp}* by gpEvolvR in *C. glutamicum*

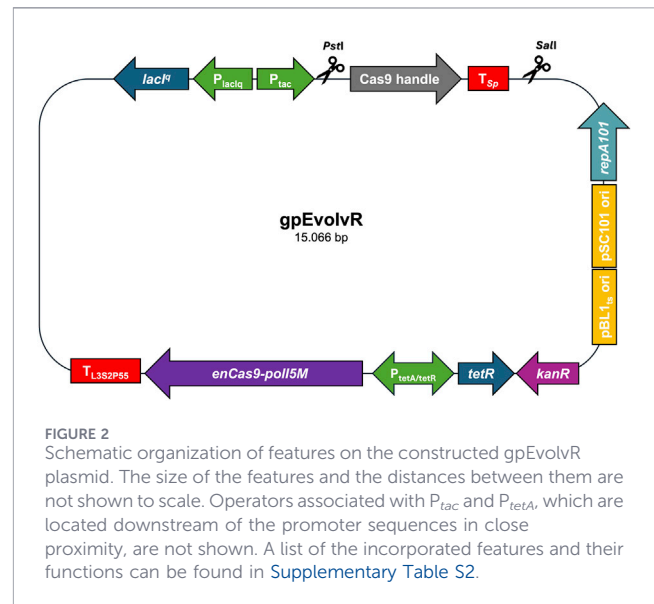
A 10 mL $\text{CGXII}_{\text{opt/Km25}}$ culture of *C. glutamicum* BETA4 $\Delta\text{actA}::\text{P}_{\text{Syn}}\text{-crtW}_{\text{Fp}}$ cells containing 60 mM acetate and 20 mM glucose as carbon sources was inoculated from LB_{Km25} -agar plates. After 24 h of incubation, expression of the EvolvR fusion protein and the sgRNA was induced by supplementation of 0.25 $\mu\text{g mL}^{-1}$ aTc and 1 mM IPTG respectively and cultivation continued for another 24 h. Cells were diluted to an $\text{OD}_{600\text{nm}}$ of 1×10^{-5} and 100 μL of the cell suspension was plated onto $\text{CGXII}_{\text{opt/Km25}}$ agar plates (Göttl et al., 2024) containing 60 mM acetate and 20 mM glucose as carbon sources.

Plates were incubated at 37 °C for plasmid curing via the pBL1_{ts} origin of replication (Nakamura et al., 2006) and an optical screening was performed after 2–4 days of incubation. Selected clones were transferred to both a $\text{CGXII}_{\text{opt}}$ agar plate without antibiotics and one with 25 $\mu\text{g mL}^{-1}$ kanamycin to verify the loss of the gpEvolvR plasmid. Clones sensitive to kanamycin were optically re-screened after 24–72 h of incubation and high-fidelity cPCR using the primers 051P/052P for *crtW_{Fp}* and V680/V099 for *crtY_{Pa}* respectively was performed on selected clones. Prepared amplicons were subjected to Sanger sequencing to detect possible mutations.

2.7 Chromosomal mutant construction of *C. glutamicum* genome via homologous recombination using *pK19mobsacB*

For the integration of genes into the *actA* (*cg2840*) locus of the *C. glutamicum* genome, both 1 kb upstream and downstream flanking regions of the *actA* locus were amplified via PCR from genomic DNA, while inserts were amplified from plasmids $\text{pECXT-P}_{\text{Syn}}\text{-crtW}_{\text{Fp}}$, $\text{pECXT-P}_{\text{tetR}}\text{-crtW}_{\text{Fp}}$. In case of P_{H36} , the promoter was synthetically introduced via oligoextension with the primer pair 058P/059P. Primers with specific overhangs were used to generate compatible ends between the *pK19mobsacB* backbone, the flanking regions, and the inserts, respectively.

A Gibson assembly (Gibson et al., 2009) was performed using the prepared *Bam*HI-restricted and dephosphorylated *pK19mobsacB* backbone. The assembled construct was transformed into chemically competent *E. coli* DH5 α cells for plasmid amplification. After verification of plasmid uptake via cPCR, plasmid DNA was isolated, and relevant regions were sequenced to confirm correct assembly. Confirmed plasmids were electroporated into electrocompetent *C. glutamicum* cells, and transformants were selected on BHIS (kanamycin 25 $\mu\text{g mL}^{-1}$) agar at 30 °C for 2 days. Clones were subsequently screened on LB (kanamycin 25 $\mu\text{g mL}^{-1}$ and sucrose 100 g L^{-1}) and LB



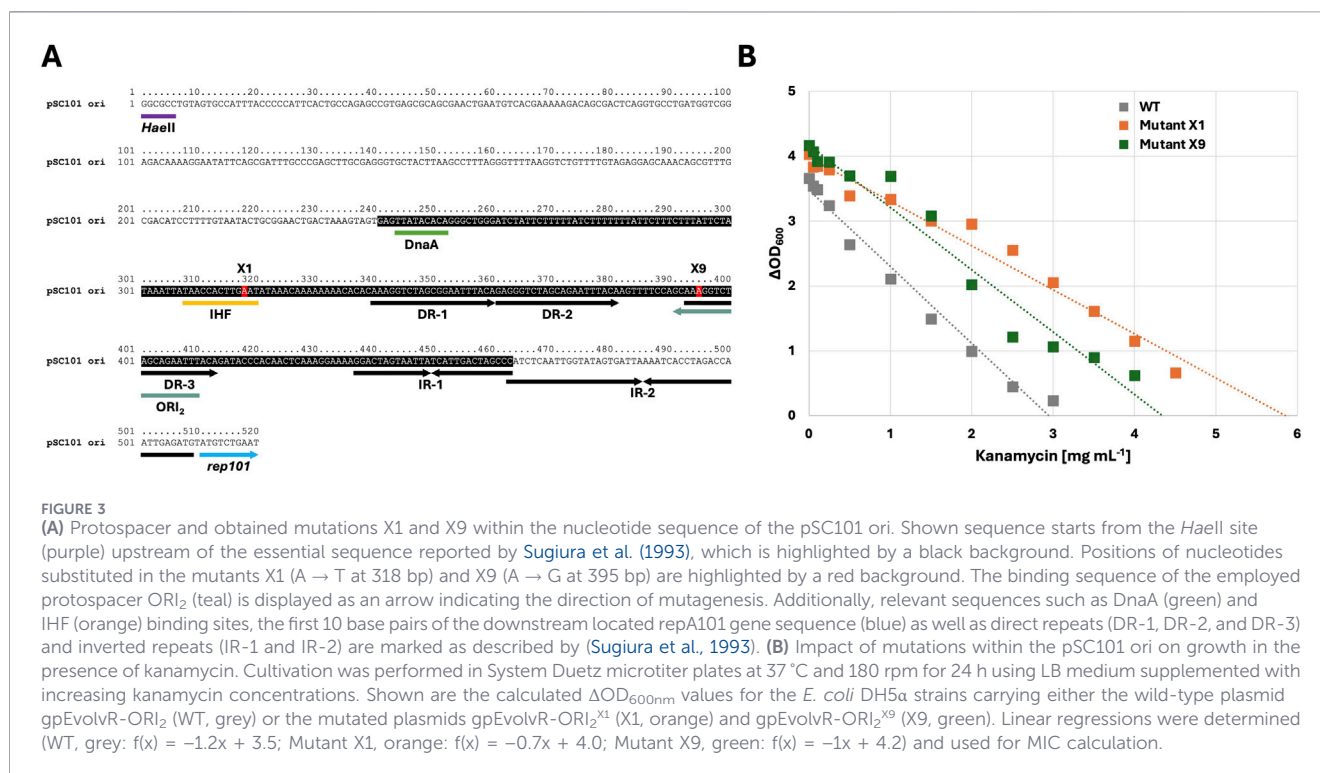
(kanamycin 25 $\mu\text{g mL}^{-1}$) plates to identify kanamycin-resistant, sucrose-sensitive colonies, which were further streaked on LB (sucrose 100 g L^{-1}) to select for the second recombination event. Kanamycin-sensitive, sucrose-resistant clones were finally verified by cPCR using primers 055P and 056P and the correct genomic integrations were confirmed by sequencing with primers 063P, V201, V209 and 1023.

2.8 Production experiments with *crtW_{Fp}* mutant variants

To assess *crtW_{Fp}* mutants under production conditions, the *crtW_{Fp}* gene was amplified from selected mutant strains via high-fidelity PCR using the primers 103P and 102P, adding overhangs for integration into *Bam*HI restricted *pSH1* backbone via Gibson assembly (Gibson et al., 2009). Assembled constructs were transformed into chemically competent *E. coli* DH5 α cells and plasmid uptake was verified by cPCR using the primers 1129 and 1135. The plasmids of positive clones were isolated and Sanger sequencing confirmed the sequence of mutant *crtW_{Fp}*.

To compare the activity of mutant *crtW_{Fp}* alone and in combination with *crtZ_{Fp}*, the plasmids were electroporated into both *C. glutamicum* BETA4 and *C. glutamicum* BETA4 ($\text{pECXT-P}_{\text{Syn}}\text{-crtZ}_{\text{Fp}}$) cells. For verification of correct transformation, high-fidelity cPCR was performed on transformants using the primers 1129/1135 and Sanger sequencing was performed on prepared amplicons using the primers 1129/1135/V201/V209.

Precultures of cloned mutant strains and corresponding reference strains were grown in 10 mL LB medium supplemented with 10 g L^{-1} glucose overnight. Technical triplicates of main cultures were grown in 10 mL $\text{CGXII}_{\text{opt}}$ minimal medium (Göttl et al., 2024) supplemented with 40 g L^{-1} of glucose and appropriate antibiotics after washing twice in 10 mL sterile TN-buffer and resuspending the cells in prepared minimal medium for inoculation to an initial $\text{OD}_{600\text{nm}}$ of 1. After 72 h of cultivation, the optical densities were measured using a Spectrophotometer V-1200 (VWR International, Leuven,



Belgium) and 500 μ L of the cell suspension were centrifuged at $20,238 \times g$ and the pellet was frozen at -20 °C until extraction and analysis.

2.9 Extraction and quantification of carotenoids

The extraction of carotenoids was carried out by resuspension of the cell pellet in 1000 μ L of a methanol:acetone (7:3; [v/v]) mixture containing butylated hydroxytoluene (BHT) as an antioxidant. Resuspended cells were shaken for 30 min at 1000 rpm and 60 °C using a ThermoMixer® C (Eppendorf SE, Hamburg, Germany), followed by centrifugation at $20,238 \times g$ for at least 10 min. The supernatant was transferred to glass vials, and the carotenoid content was quantified via high-performance liquid chromatography (HPLC) according to the protocol described by (Göttl et al., 2023).

3 Results

3.1 Design and construction of gpEvolvR

The new plasmid gpEvolvR (Figure 2) was constructed by recombining features from pEvolvR-*enCas9-poll5M*, pJYS3_easy cloning, and pS_dCas9 (Supplementary Table S2). The combination of these features enables a targeted mutagenesis approach based on a plasmid replicating in both *E. coli* and *C. glutamicum* as hosts that offers aTc inducible expression of *enCas9-poll5M* (Halperin et al., 2018) and IPTG-inducible Cas9 handle expression and that is curable via temperature sensitive origin of replication pBL1_{ts} (Nakamura et al., 2006). Protospacer DNAs can be integrated via *PstI* restriction followed by Gibson assembly

(Gibson et al., 2009), and the system is prepared for multiplex mutagenesis through integration of multiple sgRNA expression cassettes as described by (Sakuma et al., 2014) (Figure 2).

3.2 *In vivo* mutagenesis of the pSC101 ori by gpEvolvR

EvolvR was developed for application in *E. coli*, with replication of the pEvolvR-*enCas9-poll5M* plasmid being initiated by the oriV origin of replication derived from plasmid pBR322 (Halperin et al., 2018). To show that the recombined plasmid gpEvolvR is still stable and EvolvR active in its original host after the exchange of the origin of replication to the pSC101 ori donated by pJYS3_easy cloning (Supplementary Table S2), a mutagenesis experiment was performed in *E. coli* DH5 α cells with the pSC101 ori on gpEvolvR as the target. A corresponding protospacer (ORI₂; Supplementary Table S1), targeting a directed repeat sequence (DR-3) of the pSC101 ori (Figure 3), was integrated upstream of the sgRNA scaffold of gpEvolvR.

After mutagenesis in *E. coli* DH5 α using the gpEvolvR-ORI₂ construct, 11 colonies were isolated from LB agar plates containing 1 mg mL⁻¹ kanamycin and subjected to sequencing analysis. The gpEvolvR-ORI₂^{X1} variant (short: X1) resulted from an A → T base substitution located 318 bp downstream of the *HaeII* site within the binding sequence of the integration host factor (IHF) (Figure 3). Nine of the analyzed clones carried the X1 variant of pSC101 ori. The second identified variant gpEvolvR-ORI₂^{X9} (short: X9) resulted from an A → G base substitution located 395 bp downstream of the *HaeII* site within the sequence of the third direct repeat (DR-3) within the pSC101 ori (Figure 3A). Moreover, one isolated clone was able to grow under the applied selective conditions, but did not harbor a mutation within the *ori* region.

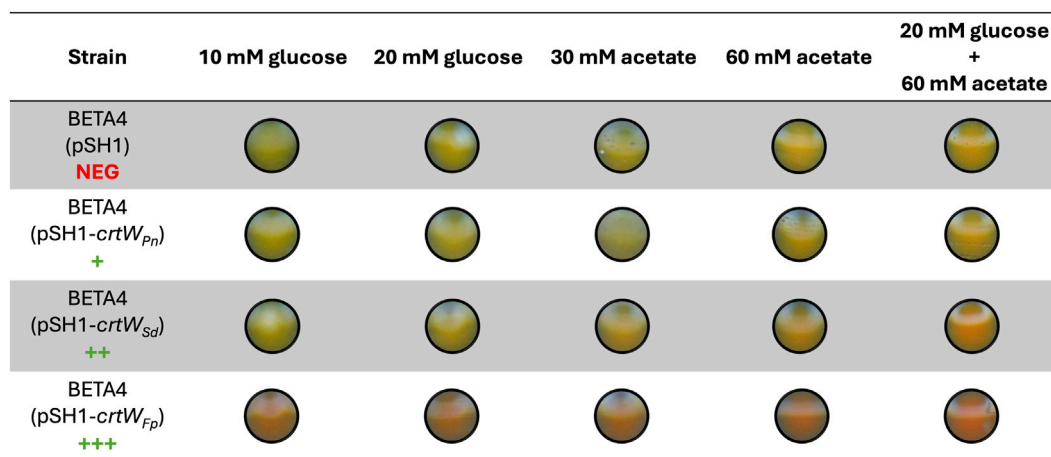


FIGURE 4

Pigmentation of single colonies from *Corynebacterium glutamicum* BETA4 strains expressing *crtW* variants on CGXII_{opt/Km25} agar plates containing different carbon source compositions. As carbon sources glucose (10 mM and 20 mM) as well as its carbon-equivalent concentrations of acetate (30 mM and 60 mM) and a combination of both (20 mM glucose and 60 mM acetate) were used. The corresponding empty vector strain *Corynebacterium glutamicum* BETA4 (pSH1) served as a reference (NEG) to the strains expressing *crtW* variants which are sorted for their activity in *Corynebacterium glutamicum* (+, ++, and +++) as reported by (Göttl et al., 2023). Plates were incubated at 30 °C for 2 days followed by incubation at room temperature for another 4 days.

Since mutations in the pSC101 ori can be expected to influence plasmid copy number and consequently affect host resistance levels through gene dosage effects in this case of the kanamycin resistance (Potekhin and Danilenko, 1985), growth experiments were carried out using increasing concentrations of kanamycin. Since a previous E-Test on LB agar plates was not sufficient to observe any inhibitory effects by kanamycin on the strains carrying the gpEvolvR-ORI₂ variants (Supplementary Figure S1), an experiment using liquid medium in System Duetz microtiter plates was performed.

The examined mutants X1 and X9 showed an increased resistance towards kanamycin (Figure 3B). Notably, the MIC values of mutant X9 (4.2 mg mL⁻¹) and mutant X1 (5.7 mg mL⁻¹) were approximately 44% and 96% higher as in the control strain (MIC: 2.9 mg mL⁻¹).

3.3 Establishment of a CrtW screening method for EvolvR experiments

In astaxanthin biosynthesis, the β-carotene ketolase (see Supplementary Figure S2) is oftentimes considered as a bottleneck (Li et al., 2020; Tao et al., 2006; Ye et al., 2006) and was thus chosen for EvolvR experiments. First, screening conditions had to be established. The ketolization of orange-colored β-carotene into the red-colored pigments echinenone and canthaxanthin produces easily detectable color changes for visual screening (Figure 1). The use of CGXII_{opt} agar medium was chosen to mimic production conditions and to reduce background pigmentation, as CGXII_{opt} itself does not exhibit any coloration similar to the relevant carotenoids β-carotene, echinenone, or canthaxanthin (Figure 1). First the optimal supplementation of carbon sources for the production of these relevant carotenoids on CGXII_{opt} agar plates needed to be determined. Therefore *C. glutamicum* BETA4 strains expressing heterologous *crtW* variants were cultivated on CGXII_{opt/Km25} agar plates supplemented with

different carbon source compositions (Figure 4; Supplementary Figure S3). The resulting colony pigmentation was used as an indirect measure of carotenoid production. The tested recombinant codon optimized variants *crtW_{Pn}* (from *Paracoccus* N81106), *crtW_{Sd}* (from *Sphingomonas* DC18) and *crtW_{Fp}* (from *Fulvamarina pelagi*) in ascending order exhibit different β-carotene ketolase production profiles in *C. glutamicum* BETA4 (data not shown) allowing the optical assessment of characteristic pigment ratios.

The single colonies of the assessed strains showed variations in pigmentation as expected (Figure 4). While the empty vector strain and the *crtW_{Pn}* variant exhibited only a yellow to bright orange coloration, increasing levels of red pigmentation could be observed for the *crtW_{Sd}* and the *crtW_{Fp}* variants respectively. Also, noticeable differences in pigmentation occurred, if the composition of the provided carbon source was altered, with increasing amounts of carbon source also causing an increase in pigmentation. Furthermore, carbon-equivalent concentrations of acetate appeared to be superior regarding the promotion of pigmentation (Supplementary Figure S3; Figure 4). The most vivid coloration of colonies for all tested strains was achieved by the combined supplementation of 20 mM glucose and 60 mM acetate as carbon sources to CGXII_{opt} agar plates, hence this combination was used for all further screening experiments.

To test if single colonies within a heterogenous group could be visually distinguished from each other as necessary for a successful screening, a mixture of the strains expressing the *crtW* variants and their respective empty vector reference strain were cultivated on CGXII_{opt/Km25} agar plates supplemented with 20 mM glucose and 60 mM acetate (Figure 5).

The colonies of the *C. glutamicum* BETA4 strain expressing *crtW_{Fp}* could be isolated easily due to their prominent red pigmentation (Figure 5), whereas the differentiation between the other variants proved to be difficult. Some colonies showed a rather

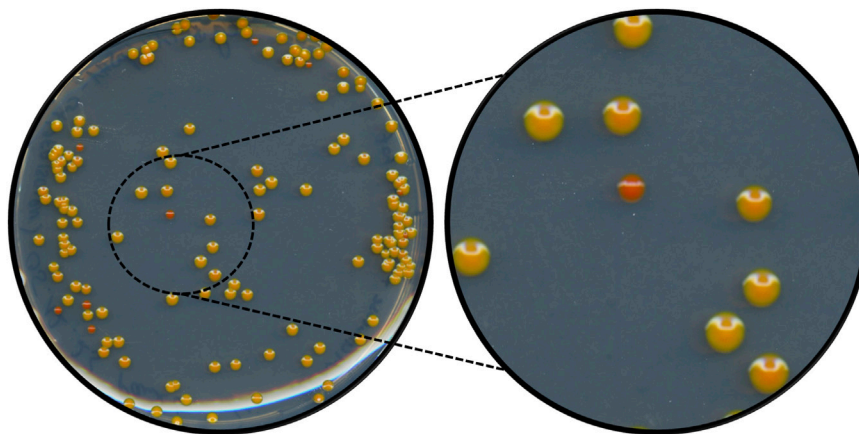


FIGURE 5 Mixture of single colonies from *Corynebacterium glutamicum* BETA4 strains expressing heterologous *crtW* variants. Cells were cultivated on CGXII_{opt/Km25} agar plates supplemented with 20 mM glucose and 60 mM acetate for 2 days at 30 °C followed by another 4 days at room temperature. The strains were mixed at a defined ratio of 40% pSH1 empty vector strain, 30% *crtW*_{PN}, 20% *crtW*_{SD} and 10% *crtW*_{FP} respectively.

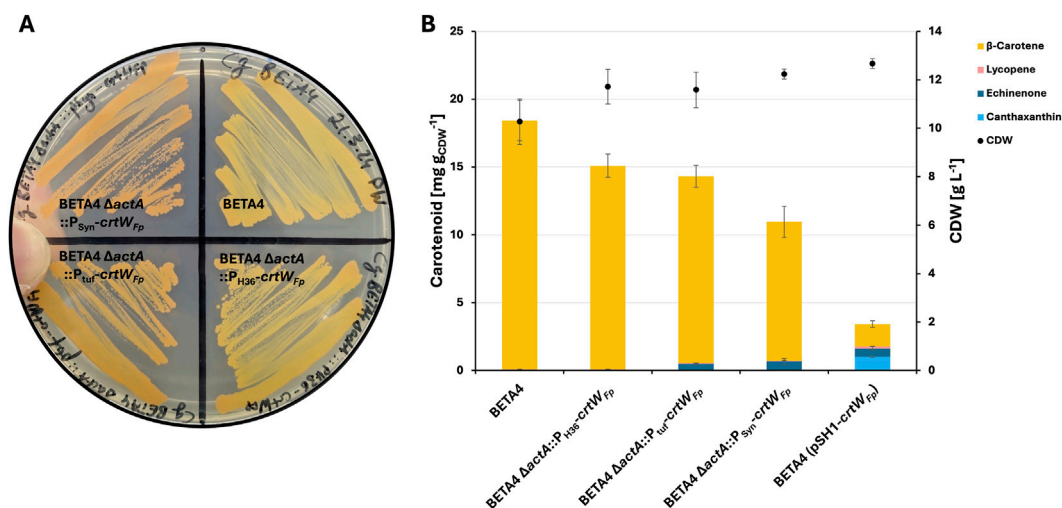


FIGURE 6 (A) Pigmentation of *Corynebacterium glutamicum* BETA4 $\Delta actA::crtW_{FP}$ integration strains with *crtW_{FP}* under the control of promoters of different strengths. Shown are the base strain BETA4 (top right) as well as the integration strains with P_{H36} promoter (bottom right), P_{tuif} promoter (bottom left) and P_{Syn} promoter (top left). Strains were streaked from glycerol stocks onto an LB agar plate and incubated at 30 °C for 48 h. (B) HPLC analysis and biomass concentration of *C. glutamicum* BETA4 $\Delta actA::crtW_{FP}$ integration strains with *crtW_{FP}* under the control of promoters of different strengths. Shown are the means of cell dry weight (CDW) and detected carotenoids relative to the CDW for 10 mL technical triplicates grown in CGXII_{opt} minimal medium supplemented with 40 g L⁻¹ glucose (and kanamycin for pSH1 harboring strains) for 48 h with the respective standard deviation as Y-error.

intense orange coloring similar to the pigmentation of the *crtW*_{SD} variant, whereas the *crtW*_{PN} variant and the empty vector reference remained indistinguishable as in Figure 4.

3.4 Construction of target strains for *crtW*_{FP} mutagenesis

As a direct relationship between genotype and phenotype is necessary to isolate single mutant *crtW*_{FP} sequence variants after mutagenesis, a respective target strain with a genomic integration of the *crtW*_{FP} gene resulting in a single copy of the target gene per cell had to be constructed. To assess different expression levels of *crtW*_{FP}

regarding their suitability for screenings, three integration strains with individual promoters of different expression strengths were constructed by pK19*mobsacB* mediated homologous recombination. The three selected promoters were already examined for episomal expression in *C. glutamicum* (Henke et al., 2021) and range from low (P_{H36}) (Yim et al., 2013) over medium (P_{tuif}) (Becker et al., 2005) to high (P_{Syn}) (Rytter et al., 2014) levels of expression. As expected, the intensity of red pigmentation caused by *CrtW*_{FP} products increases with promoter strength (Figure 6A).

The HPLC results of a production experiment (Figure 6B) confirmed the correlation between *CrtW*_{FP} products and

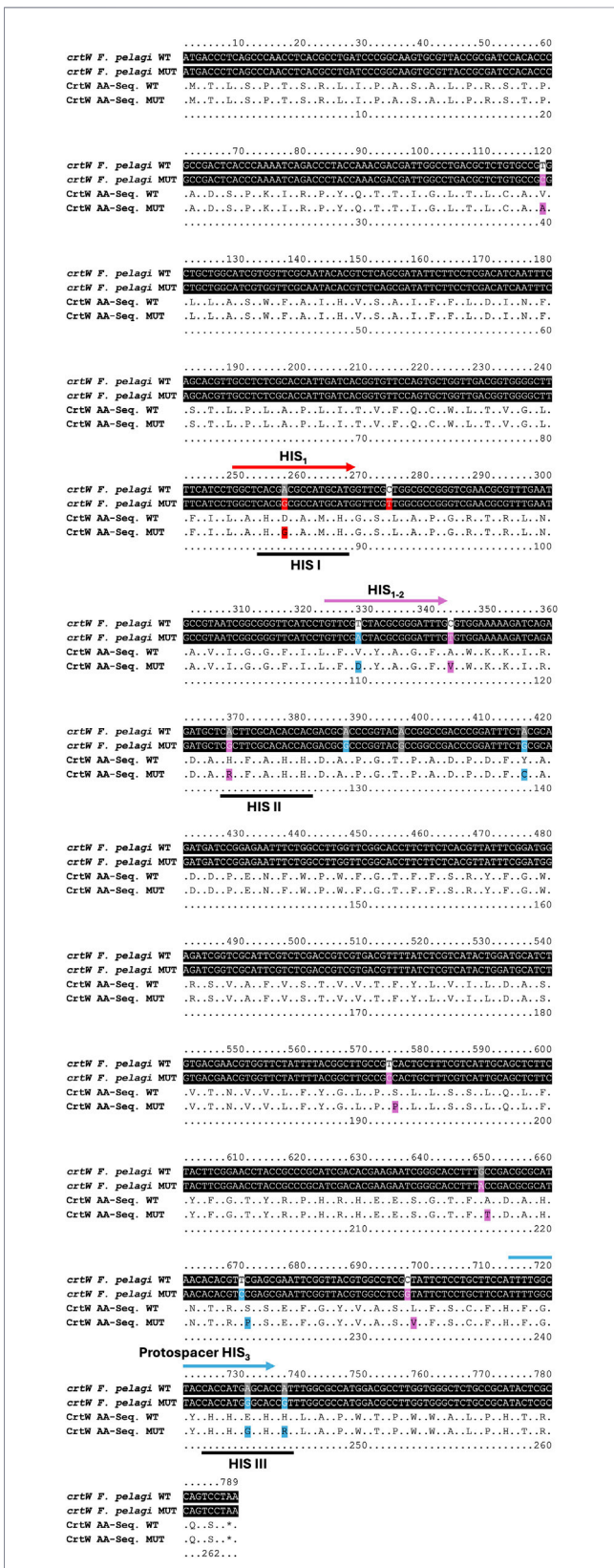


FIGURE 7
Positions of identified single nucleotide polymorphisms (SNPs) in *crtW_{Fp}* relative to the protospacer sequences employed for mutagenesis with gpEvolVR. Hypothetical nucleotide and amino acid sequences of *crtW_{Fp}* containing all identified SNPs (*crtW F. pelagi* (Continued)

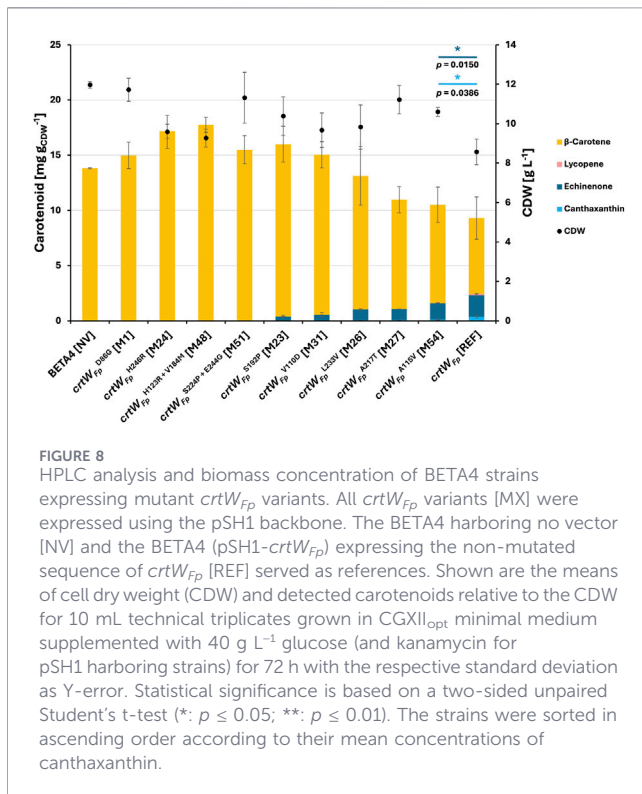
FIGURE 7 (Continued)
MUT and CrtW AA-Seq. MUT) were aligned with the corresponding wild-type sequences (*crtW F. pelagi* WT and CrtW AA-Seq. WT) using *Clustal Omega* (Madeira et al., 2024) and *Boxshade* (URL: <https://junli.netlify.app/apps/boxshade/>). Generated SNPs as well as substitutions of amino acids were highlighted in the same colors as the employed protospacer sequence (HIS₁ = red; HIS₁₋₂ = purple; HIS₃ = blue). In order to better classify the spatial localization of the substitutions within the enzyme, its histidine-rich regions were additionally marked (HIS I-III).

pigmentation, with echinenone being the main pigment produced by the integration strains. The amount of echinenone produced was similar when comparing episomal expression and genomic integrations of *crtW_{Fp}* under the control of the P_{tuf} or P_{Syn} promoter. However, remarkable amounts of canthaxanthin were only produced by episomal expression (Supplementary Table S3). Although the episomal expression strain BETA4 (pSH1-*crtW_{Fp}*) is superior in terms of CrtW_{Fp} product formation, its total amount of carotenoids is dramatically reduced compared to the other strains. In fact, the data suggests a noticeable correlation between the formation of CrtW_{Fp} products and total carotenoid content ($R^2 = 0.946$), as there is a trend of β -carotene content being more reduced than one would expect solely from its metabolism towards echinenone and canthaxanthin (Figure 6B). For example, the strain BETA4 (pSH1-*crtW_{Fp}*) showed an increase of 0.93 mg g_{CDW}⁻¹ in CrtW_{Fp} products, but a decrease of 7.54 mg g_{CDW}⁻¹ in its overall carotenoid content, with β -carotene being the major compound affected (Supplementary Table S3).

Since the strain BETA4 Δ actA::P_{Syn}-*crtW_{Fp}* expressing *crtW_{Fp}* via the P_{Syn} promoter can be easily distinguished from the parental strain BETA4 or later dysfunctional *crtW_{Fp}* mutants on plates (Figure 6A) and leaves room for mutagenic improvement compared to the pigmentation and carotenoid content observed with episomal expression (Figure 6), this variant was chosen as the target strain for the mutagenic experiments.

3.5 In vivo mutagenesis of *crtW_{Fp}* by gpEvolVR

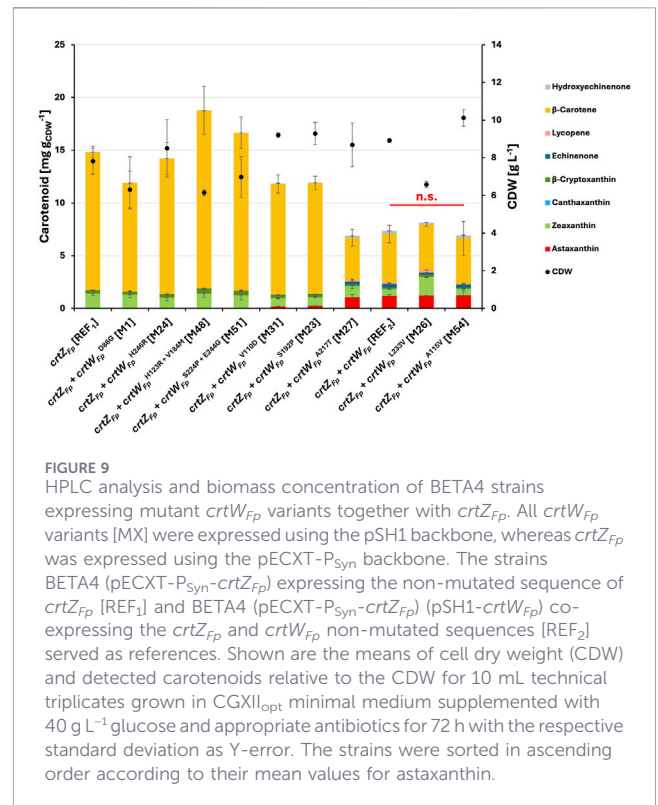
Regarding their amino acid sequence, histidine-rich regions (HIS-regions) conserved across multiple species (Supplementary Figure S2) are described for β -carotene ketolases (Ye et al., 2006). These regions are also typical for mechanistically related membrane desaturases (Shanklin et al., 1994) and are suspected to be involved in iron coordination (Arnold and Haymore, 1991) for the oxygen insertion process catalyzed by β -carotene ketolases (Bouvier et al., 1998). In accordance with this hypothesis, increased availability of iron also led to increased activity of the iron-dependent β -carotene ketolase from *F. pelagi* (CrtW_{Fp}) (Meyer et al., 2025). Furthermore, alanine scanning mutagenesis revealed that six out of eight cytosolic histidine residues within these motifs of the β -carotene ketolase from *Paracoccus* sp. N81106 (CrtW_{Pn}) are essential for its activity (Ye et al., 2006). Thus, it can be hypothesized that improving the steric accessibility of these histidine residues to iron through mutagenesis of adjacent sequence segments could yield enzyme



variants with enhanced catalytic activity. Therefore, mutagenesis efforts focused on proximal sequences next to the histidine-rich regions (Supplementary Figure S2) (Figure 7). Three protospacers were independently cloned into gpEvolvR and the resulting constructs were transformed into *C. glutamicum* BETA4 Δ actA::P_{Syn}-*crtW_{Fp}*.

Following the mutagenesis protocol described, visual differences in colony pigmentation were observed (Supplementary Figure S4). Colonies showing color deviations from the initial strain were preferentially selected for curing of the gpEvolvR derivatives (Supplementary Figures S4,S5), and the resulting plasmid-free clones were scanned for documentation (Supplementary Figures S5,S6). To identify mutations responsible for altered pigmentation, both the *crtW_{Fp}* and the *crtY_{Pa}* gene were sequenced. The appearance of pink-colored colonies alongside red and orange variants (Supplementary Figure S4) suggested an impairment of CrtY_{Pa}, which catalyzes the double cyclization of lycopene to β -carotene (Figure 1). HPLC analysis of mutant strains cultivated in 10 mL LB cultures for ~24 h was performed for carotenoid quantification. The sequencing and HPLC results are shown in Supplementary Table S4.

Sequencing revealed various mutations within the *crtW_{Fp}* and *crtY_{Pa}* genes causing alterations within their encoded amino acid sequences compared to the reference strain (REF) *C. glutamicum* BETA4 Δ actA::P_{Syn}-*crtW_{Fp}* (Figure 7). Certain mutations, such as the L233V substitution in *crtW_{Fp}* or even combination of mutations like in M24 and M25 arose multiple times independently. Notably, while mutants M6–8 carrying the CrtW_{Fp}^{L233V} mutation exhibit similar carotenoid profiles, M26 shows a markedly different profile despite having identical *crtW_{Fp}* and *crtY_{Pa}* sequences, differing only in the sgRNA used for mutagenesis (Supplementary Table S4).



3.6 Production experiment with *crtW_{Fp}* mutant strains

To enhance expression and eliminate background effects from potential off-target mutations, *crtW_{Fp}* sequences from selected mutants with altered carotenoid profiles were cloned into pSH1. Cofactor limitations in production experiments were avoided by using CGXII_{opt} minimal medium supplemented with trace salts optimized for carotenoid production in *C. glutamicum* strains (Göttl et al., 2024).

Surprisingly, strains expressing a less active or even dysfunctional variant of the *crtW_{Fp}* gene (M1, M24, M48, M51, M23, and M31) tended to produce more β -carotene than the parental strain BETA4 (Figure 8; Supplementary Table S5). For instance, the mutants *crtW_{Fp}*^{H246R} (M24) and *crtW_{Fp}*^{H123R+V184M} (M48) produced approximately 24% or even 28% more β -carotene, respectively (Figure 8). However, episomal expression via the pSH1 backbone and the corresponding addition of kanamycin to the cultivation medium negatively affected biomass concentration, as the means of cell dry weights calculated from OD_{600nm} values were slightly reduced in these samples. In contrast, previous experiments conducted over a cultivation period of only 48 h observed the opposite effect (Figure 6).

Regarding the activity of *crtW_{Fp}*, none of the mutated variants reached the titers of the reference sequence (REF) in respect to echinenone and canthaxanthin. Already for the second-best producer expressing the *crtW_{Fp}*^{A115V} variant (M54), significantly lower levels of these CrtW_{Fp}-derived products were detected by HPLC (Figure 8).

Next, transfer of the results regarding canthaxanthin production due to *crtW_{Fp}* mutations to astaxanthin production was assessed.

Therefore, $crtW_{Fp}$ strains were transformed with the pECXT- P_{Syn} - $crtZ_{Fp}$ plasmid (Figure 9).

When $crtZ_{Fp}$ is additionally expressed, a similar production behavior can be observed (Figure 9). Variants of $crtW_{Fp}$ that already showed comparable activity to the reference sequence in previous experiments (Figure 8), produced more astaxanthin in combination with $crtZ_{Fp}$ expression than impaired variants (e.g., M31 and M23) and also showed a drastically reduced amount of total carotenoids (Figure 9). While the expression of the $crtW_{Fp}$ variants M26 and M54 led to a slightly higher absolute mean value for astaxanthin compared to the reference sequence (Supplementary Table S6), this deviation is not statistically significant. In conclusion none of the $crtW_{Fp}$ variants exhibited a significantly improved production behavior—neither when expressed alone (Figure 8; Supplementary Table S5) nor upon additional $crtZ_{Fp}$ expression (Figure 9; Supplementary Table S6).

4 Discussion

In this work the EvolvR system was successfully transferred to *C. glutamicum* through design and construction of the gpEvolvR plasmid. Its mutagenic capabilities in *C. glutamicum* as well as *E. coli* on both genomic and episomal targets were demonstrated. The new gpEvolvR system serves as a dual-inducible adaptation of the EvolvR system and the temperature-sensitive pBL1_{ts} origin of replication enables its curability.

As a proof-of-principle mutagenesis of the pSC101 ori on the gpEvolvR plasmid demonstrated that the gpEvolvR plasmid is stable in *E. coli* DH5 α via the pSC101 ori donated by pJYS3_{easy} cloning and demonstrated its ability to target itself for the diversification of nucleotides. As isolated mutants conferred an improved resistance to kanamycin as represented by the calculated minimal inhibitory concentration (MIC) it can be highlighted that the EvolvR plasmid system is an efficient tool for the evolution of nucleotide sequences for the scope of tailored phenotypes (Figure 5).

To validate the initial hypothesis that the mutations introduced by gpEvolvR caused an increase in PCN as indicated by improved antibiotic resistance, the exact PCNs for the wild-type plasmid and its mutant variants X1 and X9 need to be determined. This could be done with quantitative PCR (qPCR), relative quantification using the $2^{-\Delta\Delta CT}$ method (Livak and Schmittgen, 2001) or droplet digital PCR (ddPCR) (Hindson et al., 2011).

Since the newly constructed gpEvolvR system was designed for *C. glutamicum* targeting of a chromosomal gene involved in carotenoid biosynthesis was chosen for its validation. As an experimental starting point an appropriate plate-based screening method was established for the visual discrimination of strains exhibiting different carotenoid profiles. Enhancement of carotenoid production by acetate addition likely results from an increased pyruvate and phosphoenolpyruvate (PEP) formation with boosted conversion into glyceraldehyde 3-phosphate (GAP) through gluconeogenesis (Wendisch et al., 2000) and thus making more primary carotenoid precursors available. Benefits from balanced co-utilization were observed for astaxanthin production already (Henke and Wendisch, 2019) and attribute to a synergistic effect of catabolism of glucose and acetate in *C. glutamicum* (Gerstmeir et al., 2003), which is known to lead to higher concentrations of glycolytic intermediates.

In principle, it can be assumed that random mutagenesis of a fragile, finely tuned system such as an enzyme will primarily result in dysfunctional variants (Arnold, 1996). This is especially true for the evolution of enzymes that do not confer a direct fitness gain like those involved in the carotenoid biosynthesis in *C. glutamicum*, which can be completely abolished by gene deletions with no effect on cell growth (Heider et al., 2012). Even with selection, random mutagenesis rarely leads directly to enhanced phenotypes (Kimura, 1983). The lack of improved CrtW variants likely reflects both the limited number of screened mutants and the restriction of mutagenesis to regions flanking essential histidine motifs. Consequently, the exploratory potential of the EvolvR system could be substantially enhanced by increasing library size through high-throughput screening approaches such as FACS and by targeting a broader range of sites across the $crtW$ coding sequence.

Specifically for CrtW_{Fp} it is known that its iron-coordination (Arnold and Haymore, 1991; Ye et al., 2006) as well as the spatial arrangement of transmembrane and cytosolic domains (Shanklin et al., 1994; Ye et al., 2006) are important for its catalytic function. Thus, it is likely that mutations within the iron-coordinating HIS-regions (M24 and M48) or mutations presumably causing drastic changes to protein topology, such as the observed (M51 and M23) substitutions to proline (Glykos et al., 1999; Wychowaniec et al., 2024), led to impaired or even dysfunctional variants (Supplementary Tables S3,S4) as previously reported by (Ye et al., 2006).

However, studies investigating mutant CrtW sequences in different organisms showed partially contradictory behavior regarding the effect of sequence alternations in conserved and variable regions. For example, in *Paracoccus* sp. N81106 several mutations within the histidine motifs of CrtW were investigated with varying effects. Although, most mutations led to dysfunctional enzymes (e.g., corresponding positions to H123 and H246 in CrtW_{Fp}; see Supplementary Figure S2), others only resulted in an impairment. On the other hand, the identified H219A variant was almost unaffected even though it is conserved within the third histidine motif, whereas the substituted histidine of the H184A variant does not belong to a reported histidine motif and still had a severe impact on the catalytic activity of CrtW (Ye et al., 2006). A similar behavior can be observed for proline substitutions within the CrtW sequences of other organisms. While the P12Q (P28 in CrtW_{Fp}) substitution within CrtW of *Brevundimonas* sp. SD212 expressed in *E. coli* had an positive effect (Li et al., 2020), other substitutions of conserved prolines like P116A and P228A in *Paracoccus* sp. N81106 (P136 and P253 in CrtW_{Fp}) had a rather negative effect on the catalytic activity of CrtW (Ye et al., 2006).

H123R (M48) and H246R (M24) are the only amino acid substitutions within CrtW_{Fp} that correspond to mutations described for the β -carotene ketolases of other organisms like *Sphingomonas melonis* DC18 (Tao et al., 2006), *Brevundimonas* sp. SD212 (Li et al., 2020), and *Paracoccus* sp. N81106 (Ye et al., 2006). For all other mutations, it can be assumed that they impair the catalytic activity of β -carotene ketolases e.g., based on steric hindrance that impedes the access of histidine motifs to iron ions (Li et al., 2020), or alter electron transport (Ye et al., 2006). Therefore, if protein crystal structures are not available, random

mutagenesis represents an efficient way for the optimization of β -carotene ketolases within different organisms, emphasizing the importance of tools like gpEvolvR. In addition, as EvolvR enables targeted mutagenesis of defined loci, it would even benefit from recent advances in protein structure prediction using tools such as *AlphaFold* (Jumper et al., 2021) for the rationalization of suitable target sites.

Enzyme engineering is an incremental and labor-intensive process, characterized by iterative rounds of mutagenesis with subsequent extensive screening to gradually improve the enzymes functionality (Arnold, 1998). In fact, randomized mutagenesis performed by gpEvolvR, combined with high-throughput screenings follows this stepwise optimization paradigm. Notably, implementing such diversification in a continuous rather than discontinuous manner may accelerate evolutionary progress and increase the likelihood of achieving the desired outcome more efficiently. Applying a growth-coupled selective pressure such as light stress and reactive oxygen species might favor beneficial mutations in carotenogenesis (Bhosale, 2004) but could be technically difficult to apply through self-shading effects (Saccardo et al., 2022). Alternatively, as carotenoids have an effect on membrane fluidity the effect on altered sensitivity towards osmotic stress or heat might be exploited to create a selective pressure on carotenoid biosynthesis as already demonstrated in *Arthrobacter agilis* (Fong et al., 2001) and *Staphylococcus xylosus* (Seel et al., 2020).

Halperin et al. (2018) analyzed the targeting behavior of the EvolvR system in *E. coli* using the enCas9–PolI3M fusion and observed that mutations accumulated mainly within a defined region downstream of the nick site. This pattern was consistent with strand-displacement synthesis proceeding in the 5' to 3' direction on the strand complementary to the sgRNA. Although a broader region was analyzed in their study, the core mutational activity was concentrated within a narrower window close to the nick. In addition to PolI3M, Halperin et al. (2018) described a more error-prone variant, PolI5M, which showed strongly increased mutation frequencies directly adjacent to the nick but did not display a generally expanded mutational range or elevated mutation rates at more distant positions.

In our study, we applied enCas9–PolI5M in *C. glutamicum* rather than *E. coli* and observed a shifted and less confined distribution of mutations, including substitutions upstream of the predicted nick site as well as other loci. These results suggest that the mutational pattern of EvolvR might not exclusively be influenced by the employed nickase variant itself but also by the interplay with the host organism in which the system is implemented. We analyzed the chromosomally encoded CrtY_{Pa} as a reference gene to evaluate off-targeting. Loss-of-function mutants are identifiable by pinkish colonies that rely on the accumulation of lycopene based on a non-function lycopene- β -cyclase (CrtY_{Pa}). The proline at position 190 in the amino acid sequence of CrtY_{Pa} was changed into an arginine ($\text{CrtY}_{\text{Pa}}^{\text{P190R}}$) in three independent cases (M4, M9, and M10) employing the protospacer HIS_{1-2} for mutagenesis. These three mutants exhibit nearly identical carotenoid profiles, whereas mutant M17, generated with the HIS_1 protospacer-based sgRNA carries an alanine substitution at the same position ($\text{CrtY}_{\text{Pa}}^{\text{P190A}}$) and shows dramatically different carotenoid production patterns (Supplementary Table S4). Several factors complicated the characterization of crtW_{Fp} mutants: high

redundancy of crtW_{Fp} mutations (Supplementary Table S4), potential unintended alterations to promoter sequences and crtY_{Pa} , possible additional mutations at unknown genomic positions, and suboptimal conditions for CrtW_{Fp} and CrtY_{Pa} activity in LB medium. Therefore, a selection of mutants with unique mutations and diverse carotenoid profiles was examined in the context of the parental strain under optimized conditions.

The use of catalytically dead variants of the nuclease derived from *Streptococcus pyogenes* (dCas9) are well established in *C. glutamicum* for gene expression repression via CRISPR interference (CRISPRi) (Cleto et al., 2016; Gauttam et al., 2019; Göttl et al., 2021). Despite, the application of catalytically active nuclease (Cas9) or nickase (nCas9) was found to be toxic for *C. glutamicum* (Jiang et al., 2017). This toxicity was first attributed to non-specific PAM binding of Cas9 even in the absence of complementary crRNA, which would be particularly pronounced in *C. glutamicum* as it belongs to the actinobacteria phylum with characteristically high GC content, thus offering more than 14 PAMs per 100 bp of double-stranded DNA on average for potential off-target effects (Cho et al., 2017; Jiang et al., 2017). It later became apparent that Cas9 also binds to sequences proximal to the PAM with as little as four identical nucleotides, leading to undesired off-target effects in various bacteria (Rostain et al., 2023).

Curing the entire gpEvolvR plasmid prior to visual plate screening ensures a stable relationship between genotype and phenotype. As an alternative adapting of the *tetR/tetO* induction system with a reverse-acting tetracycline repressor variant carrying the substitutions G96E and L205S (Kamionka et al., 2004; Scholz et al., 2003) might be established in the future allowing the termination of the gene expression of the enCas9–PolI5M by aTc addition at any chosen timepoint.

Cas9-based off-target effects were found to be dependent on both nuclease and sgRNA expression levels (Hsu et al., 2013; Pattanayak et al., 2013). Corresponding attempts to reduce off-target activity induced toxicity by reducing the plasmid-borne induction in *C. glutamicum* (Peng et al., 2017; Yao et al., 2021) or by employing inducible chromosome-based expression (Wang B. et al., 2018) demonstrated to be successful. While chromosomal integration of the gpEvolvR system would defeat its purpose, reducing the expression of the enCas9–PolI5M fusion protein and the sgRNA could be achieved by titrating their inducers aTc and IPTG, respectively.

Alternative EvolvR enzymes could be designed e.g., with the recently released royalty free MAD7 (*ErCas12a*) nuclease (Manus Bio Inc., Waltham, United States; formerly Inscripta). Originally derived from *Eubacterium rectale*, this Cas12a nuclease has been successfully employed for genome editing in mammalian (Wierson et al., 2019), microbial (Price et al., 2020), and plant cells (Lin et al., 2021). In fact, MAD7 has already been successfully used for engineering lycopene biosynthesis in *C. glutamicum*, increasing the yield by 102-fold compared to the parental strain (Zhan et al., 2024). Compared to *FnCpf1*, which relies on the PAM 5'-TTTN-3' (Jiang et al., 2017), MAD7 depends on the PAM 5'-YTTN-3', thus offering greater targeting flexibility in GC-rich strains like *C. glutamicum* (Zhan et al., 2024). As the EvolvR system depends on a nickase, the MAD7 nuclease could be subjected to an R1173A amino acid substitution conferring nickase activity (nMAD7) based on *AsCpf1* crystal structure experiments performed by (Yamano et al., 2016).

Data availability statement

The original contributions presented in the study are included in the article/[Supplementary Material](#), further inquiries can be directed to the corresponding author.

Author contributions

PMW: Conceptualization, Methodology, Investigation, Data curation, Formal Analysis, Writing – original draft, Writing – review and editing. VLG: Conceptualization, Methodology, Formal Analysis, Investigation, Supervision, Writing – review and editing. JS: Investigation, Data curation, Formal Analysis, Writing – review and editing. VFW: Conceptualization, Methodology, Supervision, Writing – review and editing, Funding acquisition, Resources. NAH: Conceptualization, Funding acquisition, Supervision, Writing – original draft, Writing – review and editing.

Funding

The author(s) declared that financial support was received for this work and/or its publication. This research was funded by the German Federal Ministry of Education and Research (BMBF) project KaroTec (grant number: 03VP09460). NAH acknowledges support by the KIT-Publication Fund of the Karlsruhe Institute of Technology.

Acknowledgements

We thank Ina Schmitt, Irene Krahn, and Tim Prasun for support in plasmid construction and laboratory support.

References

- Arnold, F. H. (1996). Directed evolution: creating biocatalysts for the future. *Chem. Eng. Sci.* 51 (23), 5091–5102. doi:10.1016/s0009-2509(96)00288-6
- Arnold, F. H. (1998). Design by directed evolution. *Accounts Chem. Res.* 31 (3), 125–131. doi:10.1021/ar960017f
- Arnold, F. H., and Haymore, B. L. (1991). Engineered metal-binding proteins: purification to protein folding. *Science* 252 (5014), 1796–1797. doi:10.1126/science.1648261
- Becker, J., Klopprogge, C., Zelder, O., Heinze, E., and Wittmann, C. (2005). Amplified expression of fructose 1,6-Bisphosphatase in *Corynebacterium glutamicum* increases *in vivo* flux through the pentose phosphate pathway and lysine production on different carbon sources. *Appl. Environ. Microbiol.* 71 (12), 8587–8596. doi:10.1128/AEM.71.12.8587-8596.2005
- Berman, J., Zorrilla-López, U., Farré, G., Zhu, C., Sandmann, G., Twyman, R. M., et al. (2015). Nutritionally important carotenoids as consumer products. *Phytochem. Rev.* 14 (5), 727–743. doi:10.1007/s11101-014-9373-1
- Bhosale, P. (2004). Environmental and cultural stimulants in the production of carotenoids from microorganisms. *Appl. Microbiol. Biotechnol.* 63 (4), 351–361. doi:10.1007/s00253-003-1441-1
- Blin, K., Pedersen, L. E., Weber, T., and Lee, S. Y. (2016). CRISPy-web: an online resource to design sgRNAs for CRISPR applications. *Synthetic Syst. Biotechnol.* 1 (2), 118–121. doi:10.1016/j.synbio.2016.01.003
- Boch, J., Scholze, H., Schornack, S., Landgraf, A., Hahn, S., Kay, S., et al. (2009). Breaking the code of DNA binding specificity of TAL-type III effectors. *Science* 326 (5959), 1509–1512. doi:10.1126/science.1178811
- Bornscheuer, U. T., Huisman, G. W., Kazlauskas, R. J., Lutz, S., Moore, J. C., and Robins, K. (2012). Engineering the third wave of biocatalysis. *Nature* 485 (7397), 185–194. doi:10.1038/nature11117
- Bouvier, F., Keller, Y., d'Harlingue, A., and Camara, B. (1998). Xanthophyll biosynthesis: molecular and functional characterization of carotenoid hydroxylases from pepper fruits *Capsicum annuum* L. *Biochim. Biophys. Acta, Lipids Lipid Metab.* 1391 (3), 320–328. doi:10.1016/s0005-2760(98)00029-0
- Camps, M., Naukkarinen, J., Johnson, B. P., and Loeb, L. A. (2003). Targeted gene evolution in *Escherichia coli* using a highly error-prone DNA polymerase I. *Proc. Natl. Acad. Sci.* 100 (17), 9727–9732. doi:10.1073/pnas.1333928100
- Cho, J. S., Choi, K. R., Prabowo, C. P. S., Shin, J. H., Yang, D., Jang, J., et al. (2017). CRISPR/Cas9-coupled recombineering for metabolic engineering of *Corynebacterium glutamicum*. *Metab. Eng.* 42, 157–167. doi:10.1016/j.ymben.2017.06.010
- Cleto, S., Jensen, J. V., Wendisch, V. F., and Lu, T. K. (2016). *Corynebacterium glutamicum* metabolic engineering with CRISPR interference (CRISPRi). *ACS Synth. Biol.* 5 (5), 375–385. doi:10.1021/acssynbio.5b00216
- Cong, L., Ran, F. A., Cox, D., Lin, S., Barretto, R., Habib, N., et al. (2013). Multiplex genome engineering using CRISPR/Cas systems. *Science* 339 (6121), 819–823. doi:10.1126/science.1231143
- Elena, S. F., and Lenski, R. E. (2003). Evolution experiments with microorganisms: the dynamics and genetic bases of adaptation. *Nat. Rev. Genet.* 4 (6), 457–469. doi:10.1038/nrg1088
- Fletcher, E., Chen, Y., Caspeta, L., and Feizi, A. (2022). Editorial: genomic strategies for efficient microbial cell factories. *Front. Bioeng. Biotechnol.* 10, 962828. doi:10.3389/fbioe.2022.962828
- Fong, N. J. C., Burgess, M. L., Barrow, K. D., and Glenn, D. R. (2001). Carotenoid accumulation in the psychrotrophic bacterium *Arthrobacter agilis* in response to thermal and salt stress. *Appl. Microbiol. Biotechnol.* 56 (5-6), 750–756. doi:10.1007/s002530100739

Conflict of interest

The author(s) declared that this work was conducted in the absence of any commercial or financial relationships that could be construed as a potential conflict of interest.

Generative AI statement

The author(s) declared that generative AI was not used in the creation of this manuscript.

Any alternative text (alt text) provided alongside figures in this article has been generated by Frontiers with the support of artificial intelligence and reasonable efforts have been made to ensure accuracy, including review by the authors wherever possible. If you identify any issues, please contact us.

Publisher's note

All claims expressed in this article are solely those of the authors and do not necessarily represent those of their affiliated organizations, or those of the publisher, the editors and the reviewers. Any product that may be evaluated in this article, or claim that may be made by its manufacturer, is not guaranteed or endorsed by the publisher.

Supplementary material

The Supplementary Material for this article can be found online at: <https://www.frontiersin.org/articles/10.3389/fbioe.2026.1827071/full#supplementary-material>

- Gauttam, R., Seibold, G. M., Mueller, P., Weil, T., Weiß, T., Handrick, R., et al. (2019). A simple dual-inducible CRISPR interference system for multiple gene targeting in *Corynebacterium glutamicum*. *Plasmid* 103, 25–35. doi:10.1016/j.plasmid.2019.04.001
- Gerstmeier, R., Wendisch, V. F., Schnicke, S., Ruan, H., Farwick, M., Reinscheid, D., et al. (2003). Acetate metabolism and its regulation in *Corynebacterium glutamicum*. *J. Biotechnol.* 104 (1–3), 99–122. doi:10.1016/s0168-1656(03)00167-6
- Gibson, D. G., Young, L., Chuang, R. Y., Venter, J. C., Hutchison, C. A., and Smith, H. O. (2009). Enzymatic assembly of DNA molecules up to several hundred kilobases. *Nat. Methods* 6 (5), 343–345. doi:10.1038/nmeth.1318
- Glykos, N. M., Cesareni, G., and Kokkinidis, M. (1999). Protein plasticity to the extreme: changing the topology of a 4- α -helical bundle with a single amino acid substitution. *Structure* 7 (6), 597–603. doi:10.1016/s0969-2126(99)80081-1
- Göttl, V. L., Schmitt, I., Braun, K., Peters-Wendisch, P., Wendisch, V. F., and Henke, N. A. (2021). CRISPRi-Library-Guided target identification for engineering carotenoid production by *Corynebacterium glutamicum*. *Microorganisms* 9 (4), 670. doi:10.3390/microorganisms9040670
- Göttl, V. L., Pucker, B., Wendisch, V. F., and Henke, N. A. (2023). Screening of structurally distinct lycopene β -Cyclases for production of the cyclic C40 carotenoids β -Carotene and astaxanthin by *Corynebacterium glutamicum*. *J. Agric. Food Chem.* 71 (20), 7765–7776. doi:10.1021/acs.jafc.3c01492
- Göttl, V. L., Meyer, F., Schmitt, I., Persicke, M., Peters-Wendisch, P., Wendisch, V. F., et al. (2024). Enhancing astaxanthin biosynthesis and pathway expansion towards glycosylated C40 carotenoids by *Corynebacterium glutamicum*. *Sci. Rep.* 14 (1), 8081. doi:10.1038/s41598-024-58700-9
- Halperin, S. O., Tou, C. J., Wong, E. B., Modavi, C., Schaffer, D. V., and Dueber, J. E. (2018). CRISPR-guided DNA polymerases enable diversification of all nucleotides in a tunable window. *Nature* 560 (7717), 248–252. doi:10.1038/s41586-018-0384-8
- Hanahan, D. (1983). Studies on transformation of *Escherichia coli* with plasmids. *J. Mol. Biol.* 166 (4), 557–580. doi:10.1016/s0022-2836(83)80284-8
- Hayashi, Y., Ito, T., Yoshimura, T., and Hemmi, H. (2018). Utilization of an intermediate of the methylerythritol phosphate pathway, (E)-4-hydroxy-3-methylbut-2-en-1-yl diphosphate, as the prenyl donor substrate for various prenyltransferases. *Biosci. Biotechnol. Biochem.* 82 (6), 993–1002. doi:10.1080/09168451.2017.1398064
- Heider, S. A. E., Peters-Wendisch, P., and Wendisch, V. F. (2012). Carotenoid biosynthesis and overproduction in *Corynebacterium glutamicum*. *BMC Microbiol.* 12 (1), 198. doi:10.1186/1471-2180-12-198
- Heider, S. A. E., Peters-Wendisch, P., Netzer, R., Stafnes, M., Brautaset, T., and Wendisch, V. F. (2014). Production and glucosylation of C50 and C40 carotenoids by metabolically engineered *Corynebacterium glutamicum*. *Appl. Microbiol. Biotechnol.* 98 (3), 1223–1235. doi:10.1007/s00253-013-5359-y
- Henke, N. A., and Wendisch, V. F. (2019). Improved astaxanthin production with *Corynebacterium glutamicum* by application of a membrane fusion protein. *Mar. Drugs* 17 (11), 621. doi:10.3390/md17110621
- Henke, N. A., Heider, S., Peters-Wendisch, P., and Wendisch, V. (2016). Production of the marine carotenoid astaxanthin by metabolically engineered *Corynebacterium glutamicum*. *Mar. Drugs* 14 (7), 124. doi:10.3390/md14070124
- Henke, N. A., Heider, S. A. E., Hannibal, S., Wendisch, V. F., and Peters-Wendisch, P. (2017). Isoprenoid pyrophosphate-dependent transcriptional regulation of carotenogenesis in *Corynebacterium glutamicum*. *Front. Microbiol.* 8, 633. doi:10.3389/fmicb.2017.00633
- Henke, N. A., Krahn, I., and Wendisch, V. F. (2021). Improved plasmid-based inducible and constitutive gene expression in *Corynebacterium glutamicum*. *Microorganisms* 9 (1), 204. doi:10.3390/microorganisms9010204
- Hindson, B. J., Ness, K. D., Masquelier, D. A., Belgrader, P., Heredia, N. J., Makarewicz, A. J., et al. (2011). High-throughput droplet digital PCR system for absolute quantitation of DNA copy number. *Anal. Chem.* 83 (22), 8604–8610. doi:10.1021/ac202028g
- Hsu, P. D., Scott, D. A., Weinstein, J. A., Ran, F. A., Konermann, S., Agarwala, V., et al. (2013). DNA targeting specificity of RNA-guided Cas9 nucleases. *Nat. Biotechnol.* 31 (9), 827–832. doi:10.1038/nbt.2647
- Hurtado, J. E., Schieferecke, A. J., Halperin, S. O., Guan, J., Aidlen, D., Schaffer, D. V., et al. (2025). Nickase fidelity drives EvolvR-mediated diversification in mammalian cells. *Nat. Commun.* 16 (1), 3723. doi:10.1038/s41467-025-58414-0
- Jiang, Y., Qian, F., Yang, J., Liu, Y., Dong, F., Xu, C., et al. (2017). CRISPR-Cpf1 assisted genome editing of *Corynebacterium glutamicum*. *Nat. Commun.* 8 (1), 15179. doi:10.1038/ncomms15179
- Jinek, M., Chylinski, K., Fonfara, I., Hauer, M., Doudna, J. A., and Charpentier, E. (2012). A programmable Dual-RNA-Guided DNA endonuclease in adaptive bacterial immunity. *Science* 337 (6096), 816–821. doi:10.1126/science.1225829
- Jumper, J., Evans, R., Pritzel, A., Green, T., Figurnov, M., Ronneberger, O., et al. (2021). Highly accurate protein structure prediction with AlphaFold. *Nature* 596 (7873), 583–589. doi:10.1038/s41586-021-03819-2
- Kamionka, A., Bogdanska-Urbiński, J., Scholz, O., and Hillen, W. (2004). Two mutations in the tetracycline repressor change the inducer anhydrotetracycline to a corepressor. *Nucleic Acids Res.* 32 (2), 842–847. doi:10.1093/nar/gkh200
- Kewalramani, N., Emili, A., and Crovella, M. (2023). State-of-the-art computational methods to predict protein–protein interactions with high accuracy and coverage. *Proteomics* 23 (21–22), 2200292. doi:10.1002/pmic.202200292
- Kim, Y. G., Cha, J., and Chandrasegaran, S. (1996). Hybrid restriction enzymes: zinc finger fusions to Fok I cleavage domain. *Proc. Natl. Acad. Sci.* 93 (3), 1156–1160. doi:10.1073/pnas.93.3.1156
- Kimura, M. (1983). *The neutral theory of molecular evolution*. 1st edition. Cambridge, United Kingdom: Cambridge University Press.
- Kroll, A., Ranjan, S., Engqvist, M. K. M., and Lercher, M. J. (2023). A general model to predict small molecule substrates of enzymes based on machine and deep learning. *Nat. Commun.* 14 (1), 2787. doi:10.1038/s41467-023-38347-2
- Leßmeier, L., and Wendisch, V. F. (2015). Identification of two mutations increasing the methanol tolerance of *Corynebacterium glutamicum*. *BMC Microbiol.* 15 (1), 216. doi:10.1186/s12866-015-0558-6
- Li, D., Li, Y., Xu, J.-Y., Li, Q.-Y., Tang, J.-L., Jia, S.-R., et al. (2020). Engineering CrtW and CrtZ for improving biosynthesis of astaxanthin in *Escherichia coli*. *Chin. J. Nat. Med.* 18 (9), 666–676. doi:10.1016/S1875-5364(20)60005-X
- Lin, Q., Zhu, Z., Liu, G., Sun, C., Lin, D., Xue, C., et al. (2021). Genome editing in plants with MAD7 nuclease. *J. Genet. Genomics* 48 (6), 444–451. doi:10.1016/j.jgg.2021.04.003
- Livak, K. J., and Schmittgen, T. D. (2001). Analysis of relative gene expression data using real-time quantitative PCR and the 2⁻ $\Delta\Delta$ CT method. *Methods* 25 (4), 402–408. doi:10.1006/meth.2001.1262
- Loh, E., Salk, J., and Loeb, L. A. (2010). Optimization of DNA polymerase mutation rates during bacterial evolution. *Proc. Natl. Acad. Sci.* 107 (3), 1154–1159. doi:10.1073/pnas.0912451107
- Lu, Q., Bu, Y. F., and Liu, J. Z. (2017). Metabolic engineering of *Escherichia coli* for producing astaxanthin as the predominant carotenoid. *Mar. Drugs* 15 (10), 296. doi:10.3390/md15100296
- Madeira, F., Madhusoodanan, N., Lee, J., Eusebi, A., Niewielska, A., Tivey, A. R. N., et al. (2024). The EMBL-EBI job dispatcher sequence analysis tools framework in 2024. *Nucleic Acids Res.* 52 (W1), W521–W525. doi:10.1093/nar/gkae241
- Mali, P., Yang, L., Esvelt, K. M., Aach, J., Guell, M., DiCarlo, J. E., et al. (2013). RNA-guided human genome engineering via Cas9. *Science* 339 (6121), 823–826. doi:10.1126/science.1232033
- Meyer, F., Schmitt, I., Wendisch, V. F., and Henke, N. A. (2025). Response surface-based media optimization for astaxanthin production in *Corynebacterium glutamicum*. *Front. Bioeng. Biotechnol.* 13, 1516522. doi:10.3389/fbioe.2025.1516522
- Mojica, F. J. M., Diez-Villaseñor, C., García-Martínez, J., and Almendros, C. (2009). Short motif sequences determine the targets of the prokaryotic CRISPR defence system. *Microbiology* 155 (3), 733–740. doi:10.1099/mic.0.023960-0
- Nakamura, J., Kanno, S., Kimura, E., Matsui, K., Nakamatsu, T., and Wachi, M. (2006). Temperature-sensitive cloning vector for *Corynebacterium glutamicum*. *Plasmid* 56 (3), 179–186. doi:10.1016/j.plasmid.2006.05.003
- Packer, M. S., and Liu, D. R. (2015). Methods for the directed evolution of proteins. *Nat. Rev. Genet.* 16 (7), 379–394. doi:10.1038/nrg3927
- Pattanayak, V., Lin, S., Guilinger, J. P., Ma, E., Doudna, J. A., and Liu, D. R. (2013). High-throughput profiling of off-target DNA cleavage reveals RNA-programmed Cas9 nuclease specificity. *Nat. Biotechnol.* 31 (9), 839–843. doi:10.1038/nbt.2673
- Peng, F., Wang, X., Sun, Y., Dong, G., Yang, Y., Liu, X., et al. (2017). Efficient gene editing in *Corynebacterium glutamicum* using the CRISPR/Cas9 system. *Microb. Cell Factories* 16 (1), 201. doi:10.1186/s12934-017-0814-6
- Pereira, J., and Alva, V. (2021). How do I get the most out of my protein sequence using bioinformatics tools? *Acta Crystallogr. Sect. D. Struct. Biol.* 77 (9), 1116–1126. doi:10.1107/S2059798321007907
- Peters-Wendisch, P. G., Schiel, B., Wendisch, V. F., Katsoulidis, E., Mockel, B., Sahm, H., et al. (2001). Pyruvate carboxylase is a major bottleneck for glutamate and lysine production by *Corynebacterium glutamicum*. *J. Mol. Microbiol. Biotechnol.* 3 (2), 295–300.
- Potekhin, I. A., and Danilenko, V. N. (1985). Determinant of resistance to kanamycin in *Streptomyces rimosus*: amplification in the chromosome and reversible genetic instability. *Mol. Biol.* 19 (3), 805–817.
- Price, M. A., Cruz, R., Bryson, J., Escalettes, F., and Rosser, S. J. (2020). Expanding and understanding the CRISPR toolbox for *Bacillus subtilis* with MAD7 and dMAD7. *Biotechnol. Bioeng.* 117 (6), 1805–1816. doi:10.1002/bit.27312
- Qi, L. S., Larson, M. H., Gilbert, L. A., Doudna, J. A., Weissman, J. S., Arkin, A. P., et al. (2013). Repurposing CRISPR as an RNA-guided platform for sequence-specific control of gene expression. *Cell* 152 (5), 1173–1183. doi:10.1016/j.cell.2013.02.022
- Rostain, W., Grebert, T., Vyhovskiy, D., Pizarro, P. T., Tshinsele-Van Bellinghen, G., Cui, L., et al. (2023). Cas9 off-target binding to the promoter of bacterial genes leads to silencing and toxicity. *Nucleic Acids Res.* 51 (7), 3485–3496. doi:10.1093/nar/gkad170
- Rytter, J. V., Helmark, S., Chen, J., Lezyk, M. J., Solem, C., and Jensen, P. R. (2014). Synthetic promoter libraries for *Corynebacterium glutamicum*. *Appl. Microbiol. Biotechnol.* 98 (6), 2617–2623. doi:10.1007/s00253-013-5481-x

- Saccardo, A., Bezzo, F., and Sforza, E. (2022). Microalgae growth in ultra-thin steady-state continuous photobioreactors: assessing self-shading effects. *Front. Bioeng. Biotechnol.* 10, 977429. doi:10.3389/fbioe.2022.977429
- Sakuma, T., Nishikawa, A., Kume, S., Chayama, K., and Yamamoto, T. (2014). Multiplex genome engineering in human cells using all-in-one CRISPR/Cas9 vector system. *Sci. Rep.* 4 (1), 5400. doi:10.1038/srep05400
- Sandmann, G. (1994). Carotenoid biosynthesis in microorganisms and plants. *Eur. J. Biochem.* 223 (1), 7–24. doi:10.1111/j.1432-1033.1994.tb18961.x
- Schäfer, A., Tauch, A., Jäger, W., Kalinowski, J., Thierbach, G., and Pühler, A. (1994). Small mobilizable multi-purpose cloning vectors derived from the *Escherichia coli* plasmids pK18 and pK19: selection of defined deletions in the chromosome of *Corynebacterium glutamicum*. *Gene* 145 (1), 69–73. doi:10.1016/0378-1119(94)90324-7
- Scholz, O., Köstner, M., Reich, M., Gastiger, S., and Hillen, W. (2003). Teaching TetR to recognize a new inducer. *J. Mol. Biol.* 329 (2), 217–227. doi:10.1016/s0022-2836(03)00427-3
- Schultenkämper, K., Brito, L. F., López, M. G., Brautaset, T., and Wendisch, V. F. (2019). Establishment and application of CRISPR interference to affect sporulation, hydrogen peroxide detoxification, and mannitol catabolism in the methylotrophic thermophile *Bacillus methanolicus*. *Appl. Microbiol. Biotechnol.* 103 (14), 5879–5889. doi:10.1007/s00253-019-09907-8
- Seel, W., Baust, D., Sons, D., Albers, M., Eitzbach, L., Fuss, J., et al. (2020). Carotenoids are used as regulators for membrane fluidity by *Staphylococcus xylosum*. *Sci. Rep.* 10 (1), 330. doi:10.1038/s41598-019-57006-5
- Shanklin, J., Whittle, E., and Fox, B. G. (1994). Eight histidine residues are catalytically essential in a membrane-associated iron enzyme, stearyl-CoA desaturase, and are conserved in alkane hydroxylase and xylene monooxygenase. *Biochemistry* 33 (43), 12787–12794. doi:10.1021/bi00209a009
- Shendure, J., and Aiden, E. L. (2012). The expanding scope of DNA sequencing. *Nat. Biotechnol.* 30 (11), 1084–1094. doi:10.1038/nbt.2421
- Slaymaker, I. M., Gao, L., Zetsche, B., Scott, D. A., Yan, W. X., and Zhang, F. (2016). Rationally engineered Cas9 nucleases with improved specificity. *Science* 351 (6268), 84–88. doi:10.1126/science.aad5227
- Stegemann, F., Seeger, J., Peters-Wendisch, P., Henke, N. A., and Wendisch, V. F. (2026). Production of ultraviolet A protectant C50 carotenoid decaprenoxanthin by metabolically engineered *Corynebacterium glutamicum*. *Bioresour. Technol.* 439, 133319. doi:10.1016/j.biortech.2025.133319
- Sugiura, S., Ohkubo, S., and Yamaguchi, K. (1993). Minimal essential origin of plasmid pSC101 replication: requirement of a region downstream of iterons. *J. Bacteriol.* 175 (18), 5993–6001. doi:10.1128/jb.175.18.5993-6001.1993
- Tao, L., Wilczek, J., Odom, J. M., and Cheng, Q. (2006). Engineering a β -carotene ketolase for astaxanthin production. *Metab. Eng.* 8 (6), 523–531. doi:10.1016/j.ymben.2006.06.001
- Tou, C. J., Schaffer, D. V., and Dueber, J. E. (2020). Targeted diversification in the *S. cerevisiae* genome with CRISPR-guided DNA polymerase I. *ACS Synth. Biol.* 9 (7), 1911–1916. doi:10.1021/acssynbio.0c00149
- Wang, B., Hu, Q., Zhang, Y., Shi, R., Chai, X., Liu, Z., et al. (2018). A RecET-assisted CRISPR–Cas9 genome editing in *Corynebacterium glutamicum*. *Microb. Cell Factories* 17 (1), 63. doi:10.1186/s12934-018-0910-2
- Wang, X., Khushk, I., Xiao, Y., Gao, Q., and Bao, J. (2018). Tolerance improvement of *Corynebacterium glutamicum* on lignocellulose derived inhibitors by adaptive evolution. *Appl. Microbiol. Biotechnol.* 102 (1), 377–388. doi:10.1007/s00253-017-8627-4
- Wendisch, V. F. (2020). Metabolic engineering advances and prospects for amino acid production. *Metab. Eng.* 58, 17–34. doi:10.1016/j.ymben.2019.03.008
- Wendisch, V. F., De Graaf, A. A., Sahm, H., and Eikmanns, B. J. (2000). Quantitative determination of metabolic fluxes during co-utilization of two carbon sources: comparative analyses with *Corynebacterium glutamicum* during growth on acetate and/or glucose. *J. Bacteriol.* 182 (11), 3088–3096. doi:10.1128/jb.182.11.3088-3096.2000
- Werner, F., Schwarzmann, L. S., Siebert, D., Rückert-Reed, C., Kalinowski, J., Wirth, M.-T., et al. (2023). Metabolic engineering of *Corynebacterium glutamicum* for fatty alcohol production from glucose and wheat straw hydrolysate. *Biotechnol. Biofuels Bioprod.* 16 (1), 116. doi:10.1186/s13068-023-02367-3
- Wierson, W. A., Simone, B. W., WareJoncas, Z., Mann, C., Welker, J. M., Kar, B., et al. (2019). Expanding the CRISPR toolbox with ErCas12a in zebrafish and human cells. *CRISPR J.* 2 (6), 417–433. doi:10.1089/crispr.2019.0026
- Wychowaniec, J. K., Srejber, M., Zeng, N., Smith, A. M., Miller, A. F., Otyepka, M., et al. (2024). Effects of proline substitution/inclusion on the nanostructure of a self-assembling β -sheet-forming peptide. *RSC Adv.* 14 (50), 37419–37430. doi:10.1039/d4ra07065h
- Yamano, T., Nishimasu, H., Zetsche, B., Hirano, H., Slaymaker, I. M., Li, Y., et al. (2016). Crystal structure of Cpf1 in complex with guide RNA and target DNA. *Cell* 165 (4), 949–962. doi:10.1016/j.cell.2016.04.003
- Yao, C., Hu, X., and Wang, X. (2021). Construction and application of a CRISPR/Cas9-assisted genomic editing system for *Corynebacterium glutamicum*. *AMB Express* 11 (1), 70. doi:10.1186/s13568-021-01231-7
- Ye, R. W., Stead, K. J., Yao, H., and He, H. (2006). Mutational and functional analysis of the β -Carotene ketolase involved in the production of canthaxanthin and astaxanthin. *Appl. Environ. Microbiol.* 72 (9), 5829–5837. doi:10.1128/AEM.00918-06
- Yim, S. S., An, S. J., Kang, M., Lee, J., and Jeong, K. J. (2013). Isolation of fully synthetic promoters for high-level gene expression in *Corynebacterium glutamicum*. *Biotechnol. Bioeng.* 110 (11), 2959–2969. doi:10.1002/bit.24954
- Zhan, Z., Chen, X., Ye, Z., Zhao, M., Li, C., Gao, S., et al. (2024). Expanding the CRISPR toolbox for engineering lycopene biosynthesis in *Corynebacterium glutamicum*. *Microorganisms* 12 (4), 803. doi:10.3390/microorganisms12040803
- Zhang, M., Gong, Z., Tang, J., Lu, F., Li, Q., and Zhang, X. (2022). Improving astaxanthin production in *Escherichia coli* by co-utilizing CrtZ enzymes with different substrate preference. *Microb. Cell Factories* 21 (1), 71. doi:10.1186/s12934-022-01798-1